

AD-A042 122

UNITED TECHNOLOGIES RESEARCH CENTER EAST HARTFORD CONN  
DEVELOPMENT OF A THREE-DIMENSIONAL COMBUSTOR FLOW ANALYSIS. VOL--ETC(U)  
OCT 76 H J GIBELING, H MCDONALD, W R BRILEY F33615-74-C-2028  
AFAPL-TR-75-59-VOL-2 NL

UNCLASSIFIED

| OF |  
AD  
A042122



12

*Handwritten signature*

AFAPL-TR-75-59  
Volume II

ADA 042122

# DEVELOPMENT OF A THREE-DIMENSIONAL COMBUSTOR FLOW ANALYSIS

## VOLUME II: THEORETICAL STUDIES

United Technologies Research Center  
East Hartford, Connecticut 06108

October 1976

TECHNICAL REPORT AFAPL-TR-75-59, VOLUME II  
FINAL REPORT FOR PERIOD 1 JUNE 75 - 1 OCTOBER 76

Approved for Public Release; Distribution Unlimited

AIR FORCE AERO-PROPULSION LABORATORY  
AIR FORCE WRIGHT AERONAUTICAL LABORATORIES  
AIR FORCE SYSTEMS COMMAND  
WRIGHT-PATTERSON AIR FORCE BASE, OHIO 45433

AD No. \_\_\_\_\_  
DDC FILE COPY

*Handwritten initials*  
DDC  
RECEIVED  
JUL 27 1977  
D

NOTICE

When Government drawings, specifications, or other data are used for any purpose other than in connection with a definitely related Government procurement operation, the United States Government thereby incurs no responsibility nor any obligation whatsoever; and the fact that the Government may have formulated, furnished, or in any way supplied the said drawings, specifications, or other data, is not to be regarded by implication or otherwise as in any manner licensing the holder or any other person or corporation, or conveying any rights or permission to manufacture, use, or sell any patented invention that may in any way be related thereto.

This final report was submitted by United Technologies Research Center, under Contract F33615-74-C-2028. The effort was sponsored by the Air Force Aero-Propulsion Laboratory, Air Force Systems Command, Wright-Patterson AFB, Ohio, under Project 3066, Task 306605 and Work Unit 30660529 with Dale A. Hudson, AFAPL/TBC, as Project Engineer. Henry McDonald formerly of United Technologies Research Center was technically responsible for the work.

The authors wish to acknowledge the unpublished experimental data provided by Hratch Semerjian of Pratt & Whitney Aircraft and taken under the Basic Technology Program.

This report has been reviewed by the Information Office, (ASD/OIP) and is releasable to the National Technical Information Service (NTIS). At NTIS, it will be available to the general public, including foreign nations.

This technical report has been reviewed and is approved for publication.

*Dale A. Hudson*

DALE A. HUDSON, GS-11  
Project Engineer

FOR THE COMMANDER

*Robert E. Henderson*

ROBERT E. HENDERSON  
Tech Area Manager, Combustion

Copies of this report should not be returned unless return is required by security considerations, contractual obligations, or notice on a specific document.

UNCLASSIFIED

SECURITY CLASSIFICATION OF THIS PAGE (When Data Entered)

19 REPORT DOCUMENTATION PAGE		READ INSTRUCTIONS BEFORE COMPLETING FORM
1. REPORT NUMBER AFAPL-TR-75-59 Vol II. ✓	2. GOVT ACCESSION NO.	3. RECIPIENT'S CATALOG NUMBER
4. TITLE (and Subtitle) DEVELOPMENT OF A THREE-DIMENSIONAL COMBUSTOR FLOW ANALYSIS. VOLUME II: THEORETICAL STUDIES.	5. TYPE OF REPORT & PERIOD COVERED Final Report, 1 June 1975 - 1 October 1976	6. PERFORMING ORG. REPORT NUMBER
7. AUTHOR(s) Howard J. Gibeling, Henry/McDonald, W. Roger Briley	8. CONTRACT OR GRANT NUMBER(s) F33615-74-C-2028	
9. PERFORMING ORGANIZATION NAME AND ADDRESS United Technologies Research Center 400 Main Street East Hartford, Connecticut 06108	10. PROGRAM ELEMENT, PROJECT, TASK AREA & WORK UNIT NUMBERS Project 3066 Task 306605 Work Unit 30660529	
11. CONTROLLING OFFICE NAME AND ADDRESS United States Air Force Air Force Systems Command Hq, 4950th Test Wing 4950/PMNB Wright Patterson AFB, Ohio 45433	12. REPORT DATE 1 October 1976	
14. MONITORING AGENCY NAME & ADDRESS (if different from Controlling Office) Air Force Aero-Propulsion Laboratory Air Force Wright Aeronautical Laboratories/TBC Air Force Systems Command Wright-Patterson AFB, Ohio 45433	13. NUMBER OF PAGES 52	15. SECURITY CLASS. (of this report) UNCLASSIFIED
16. DISTRIBUTION STATEMENT (of this Report) Approved for public release; Distribution unlimited.	15a. DECLASSIFICATION/DOWNGRADING	
17. DISTRIBUTION STATEMENT (of the abstract entered in Block 20, if different from Report)		
18. SUPPLEMENTARY NOTES		
19. KEY WORDS (Continue on reverse side if necessary and identify by block number)		
20. ABSTRACT (Continue on reverse side if necessary and identify by block number) A three-dimensional computational procedure is presented for calculating the coupled flow and chemistry within rectangular or axisymmetric combustors with a discrete circumferential distribution of injection ports. The compressible time-averaged Navier-Stokes equations are solved with coupled pseudo-kinetic hydrocarbon chemistry including the effects of turbulence, droplet vaporization and burning, and radiation transport. A two-equation		

DD FORM 1 JAN 73 1473

EDITION OF 1 NOV 68 IS OBSOLETE  
S/N 0102-014-6801

UNCLASSIFIED

SECURITY CLASSIFICATION OF THIS PAGE (When Data Entered)

409252

next page

UNCLASSIFIED

SECURITY CLASSIFICATION OF THIS PAGE (When Data Entered)

20.

cont

→ turbulence transport model utilizing the turbulence kinetic energy and its dissipation rate is employed via the Prandtl-Kolmogorov hypothesis to determine the turbulent viscosity. The governing equations are solved using the Multidimensional Implicit Nonlinear Time-dependent (MINT) procedure, which employs a unique linearization technique and a Douglas-Gunn alternating-direction-implicit (ADI) scheme. Calculations were made for the flow in a rectangular combustion chamber with a discrete distribution of inlet injection ports and the results are compared with the experimental data available for this configuration.



SECURITY CLASSIFICATION OF THIS PAGE (When Data Entered)

TABLE OF CONTENTS

	<u>Page</u>
LIST OF ILLUSTRATIONS . . . . .	iv
SYMBOLS . . . . .	vi
SECTION I - INTRODUCTION . . . . .	1
SECTION II - TURBULENCE MODEL . . . . .	6
Turbulence Model Equations . . . . .	6
Boundary Conditions . . . . .	10
Numerical Considerations . . . . .	13
SECTION III - SPATIAL DIFFERENCE FORMULATION . . . . .	15
SECTION IV - RESULTS AND CONCLUSIONS . . . . .	20
SECTION V - FREP COMPUTER CODE . . . . .	24
ILLUSTRATIONS . . . . .	25
REFERENCES . . . . .	48

ACCESSION for		
NTIS	White Section	<input checked="" type="checkbox"/>
DDC	Buff Section	<input type="checkbox"/>
UNANNOUNCED		<input type="checkbox"/>
JUSTIFICATION _____		
BY _____		
DISTRIBUTION/AVAILABILITY CODES		
Dist.	Avail.	SPECIAL
A		

LIST OF ILLUSTRATIONS

<u>Figure</u>		<u>Page</u>
1	General axisymmetric combustor geometry . . . . .	25
2	Experimental flameholder configuration for three dimensional rectangular combustor . . . . .	26
3	Computational region and coordinate system for three dimensional rectangular combustor . . . . .	27
4	Cross flow plane sections A, B, and C for profile plots .	28
5	Nondimensional axial velocity profiles . . . . .	29
6	Nondimensional axial velocity profiles . . . . .	30
7	Nondimensional axial velocity profiles . . . . .	31
8	Contours of constant nondimensional axial velocity in the cross-sectional plane . . . . .	32
9	Contours of constant nondimensional axial velocity in the cross-sectional plane . . . . .	33
10	Contours of constant nondimensional axial velocity in the cross-sectional plane . . . . .	34
11	Contours of constant nondimensional axial velocity in the cross-sectional plane . . . . .	35
12	Nondimensional turbulence kinetic energy profiles . . . .	36
13	Nondimensional turbulence kinetic energy profiles . . . .	37
14	Nondimensional turbulence kinetic energy profiles . . . .	38
15	Axial variation of temperature along port centerline ( $X_1 = 0.5, X_2 = 0.0$ ) . . . . .	39
16	Nondimensional temperature profiles . . . . .	40

LIST OF ILLUSTRATIONS (Continued)

<u>Figure</u>		<u>Page</u>
17	Nondimensional temperature profiles . . . . .	41
18	Nondimensional temperature profiles . . . . .	42
19	Contours of constant nondimensional temperature in the cross-sectional plane . . . . .	43
20	Contours of constant nondimensional temperature in the cross-sectional plane . . . . .	44
21	Contours of constant nondimensional temperature in the cross-sectional plane . . . . .	45
22	Comparison between predicted and experimental nitric oxide (NO) concentration profiles . . . . .	46
23	Nondimensional axial velocity profiles for two- dimensional FREP calculation . . . . .	47

LIST OF SYMBOLS

$A^+$	Van Driest damping constant, Eq. (7)
$c_1, c_2$	Coefficients in wall function, Eq. (24)
$C_\ell$	Turbulence model constant, Eq. (11)
$C_\mu, C_1, C_2$	Turbulence model constants, Eqs. (9-10)
$C'_\mu$	Turbulence model constant, Eq. (1)
$\bar{e}$	Mean flow rate of strain tensor, Eq. (4)
$k$	Turbulence kinetic energy, nondimensional
$l$	Mixing length; nondimensional
$L$	Reference length, dimensional
$n$	Normal coordinate at a surface
$Re$	Reference Reynolds number, $Re = \rho_D U_D L / \mu_D$
$Re_{\Delta x_i}$	Mesh Reynolds number for $x_i$ coordinate direction, nondimensional
$t$	Time, nondimensional
$\bar{u}$	Time-averaged velocity vector, nondimensional $\bar{u} = (u, v, w)$
$u_i$	Time-averaged $x_i$ -direction velocity component, nondimensional
$u'_i$	Instantaneous fluctuating $x_i$ -direction velocity component, nondimensional
$\tilde{u}$	Total tangential velocity component at a wall, nondimensional
$u^+$	Wall function velocity, Eq. (22); nondimensional
$u^*$	Friction velocity, Eq. (23); nondimensional
$U_D$	Reference velocity, dimensional
$x_1, x_2, x_3$	Orthogonal curvilinear coordinates, see Fig. 1, nondimensional

LIST OF SYMBOLS (Continued)

$y$	Distance to nearest wall for mixing length, Eqs. (5) and (7), nondimensional
$y^+$	Wall function coordinate, Eq. (21), nondimensional
$\kappa$	Von Karman constant
$\delta_k$	Spatial difference operators for central difference approximation to first derivatives ( $k = 1, 2, 3$ )
$\delta_k^2$	Spatial difference operators for central difference approximation to second derivatives ( $k = 1, 2, 3$ )
$\Delta$	Shear layer region thickness in Lilley's mixing length model, Eq. (6)
$\Delta x_1, \Delta x_2, \Delta x_3$	Grid spacings for the $x_1, x_2, x_3$ -directions
$\Delta$	Time step
$\epsilon$	Turbulence kinetic energy dissipation rate, nondimensional
$\epsilon_i$	Artificial viscosity for $x_i$ direction
$\phi$	Dummy symbol for any dependent variable
$\mu_{lam}$	Laminar dynamic viscosity, nondimensional
$\mu_T$	Effective turbulent viscosity, nondimensional
$\rho$	Time-averaged density, nondimensional
$\sigma_k, \sigma_\epsilon$	Turbulence exchange coefficients, Eqs. (8-9)
$\tau_w$	Wall shear stress, nondimensional; see Eq. (23)

LIST OF SYMBOLS (Continued)

SUBSCRIPTS

D	Denotes dimensional reference value
i, j, k	Grid point indices; $x_1$ , $x_2$ , $x_3$ -directions
n	Normal direction at a surface

SUPERSCRIPTS

n	Denotes time level ( $t^n$ )
---	------------------------------

## SECTION I

### INTRODUCTION

Predictions of gas turbine combustor performance and pollutant emission characteristics require modeling procedures possessing a high degree of sophistication. Past attempts at modeling combustion systems have been largely frustrated by the complexity of the coupled hydrodynamic and chemical processes. The difficulty can be largely attributed to the lack of understanding of the flow processes which, through the exchange of heat, mass and momentum, can directly relate to pollutant formation and combustion efficiency. For example, swirling flow has been shown to have an important influence on the stability and combustion intensity of flames (Ref. 1) as well as on residence-time distributions (Ref. 2) in combustors which, in turn, can be related to combustor performance and efficiency as well as to emission characteristics (Refs. 3 and 4). Techniques employed in modeling combustor flow processes have generally been highly simplified, particularly flow modeling techniques where stirred reactor concepts and one-dimensional assumptions are employed (Refs. 5 through

- 
1. Beer, J. M. and N. A. Chigier: Stability and Combustion Intensity of Pulverized Coal Flames - Effect of Swirl and Impingement. Journal of the Institute of Fuel, December 1969.
  2. Beer, J. M. and W. Leucker: Turbulent Flames in Rotating Flow Systems. Paper No. Inst. F-NAFTC-7, North American Fuel Technology Conference, Ottawa, Canada, (1970).
  3. Beer, J. M. and J. B. Lee: The Effects of Residence Time Distribution on the Performance and Efficiency of Combustors. The Combustion Institute, pp. 1187-1202, (1965).
  4. Marteney, P. J.: Analytical Study of the Kinetics of Formation of Nitrogen Oxide in Hydrocarbon - Air Combustion. Combustion Science and Technology, Vol. 1, pp. 37-45, (1970).
  5. Fletcher, R. S. and J. B. Heywood: A Model for Nitric Oxide Emission From Aircraft Gas Turbine Engines. AIAA Paper 71-123, (1971).
  6. Hammond, D. C., Jr. and A. M. Mellor: Analytical Predictions of Emissions from and Within an Allison J-33 Combustor. Combustion Science and Technology, Vol. 6, pp. 279-286, (1973).
  7. Hammond, D. C., Jr. and A. M. Mellor: Analytical Calculations for the Performance and Pollutant Emissions of Gas Turbine Combustors. Combustion Science and Technology, Vol. 4, pp. 101-112, (1971).
  8. Roberts, R., L. D. Aceto, R. Keilback, D. P. Teixeira, and J. M. Bonnell: An Analytical Model for Nitric Oxide Formation in a Gas Turbine Combustion Chamber. AIAA Paper No. 71-715, (1971).

10). Chemistry is frequently modeled by assuming equilibrium hydrocarbon fuel decomposition and two phase flow effects are seldom considered. In some more recent modeling attempts, for example, Fletcher and Heywood (Ref. 5) and Hammond and Mellor (Refs. 6 and 7), the stirred reactor concept is employed to assess the effect of residence-time on combustion behavior and to predict pollutant emissions in gas turbines. Droplet vaporization and burning were neglected in these studies; however, a quasi-global finite-rate hydrocarbon combustion mechanism was employed by Hammond and Mellor to model the chemistry. In related work, Roberts, et al., (Ref. 8), in an attempt to predict nitrogen oxide formation in gas turbine combustors, subdivided the combustor into three regions: one corresponding to the central recirculation portion of the upstream zone; a second representing the flow region surrounding the recirculation zone which was interpreted to be a one-dimensional reacting zone; and the third downstream zone modeled as a one-dimensional region. Both finite-rate and equilibrium hydrocarbon chemistry models were considered. It is interesting that little difference in the predicted NO levels was noted in their results between the equilibrium and finite-rate hydrocarbon cases. A more recent analysis directed toward low power application by Mosier, et al., (Ref. 9) basically extended the work of Ref. 8 through the use of a more sophisticated finite-rate hydrocarbon chemistry model obtaining trends in agreement with experimental data. The modular approach proposed by Edelman and Economos (Ref. 10) is an attempt at formulating a general analytical procedure for predicting combustor behavior by treating the various critical combustor processes on an individual basis or coupled as a function of operating conditions. Difficulty with the approach lies with its method of accounting for recirculation (a stirred reactor is presently used) and its inability to provide a unified description of the burner under a given set of operating conditions.

The foregoing methods are lacking primarily in their ability to properly account for mixing phenomena occurring in the reverse flow recirculation regions of combustion devices. It has recently become feasible, however, to treat more rigorously flows having recirculation zones, by numerical solution

- 
9. Mosier, S. A., R. Roberts, and R. E. Henderson: Development and Verification of an Analytical Model for Predicting Emissions from Gas Turbine Engine Combustors During Low Power Operation. 41st Meeting Propulsion and Energetics Panel of AGARD, (1973).
  10. Edelman, R. and C. Economos: A Mathematical Model for Jet Engine Combustor Pollutant Emissions. AIAA Paper No. 71-714, (1971).

of elliptic equations governing combustng flows. For example, one such numerical method based on an explicit point-by-point relaxation procedure has been suggested by Gosman, et al., (Ref. 11). Subsequently, the Imperial College group has developed a line relaxation procedure for solution of elliptic partial differential equations (Refs. 12 and 13). Several applications of this procedure to combustng flows have been made in recent years with emphasis on the influence of both combustion chemistry models and turbulent fluctuations (Refs. 14 and 15).

For several years improved numerical procedures have been under development at UTRC for solving combustng flows containing recirculation zones. One of these UTRC procedures is an implicit computational scheme, and is novel in that residuals are relaxed simultaneously throughout the entire flow field, rather than one at a time, as in the explicit point methods, or a line at a time as in the line methods. Under a joint AFAPL/FAA contract, the UTRC Field Relaxation Elliptic Procedure (FREP) based on the rigorous solution of the governing equations was further developed and used to predict the performance and emission characteristics of can-annular and annular gas turbine combustors (Ref. 16). Further development of the procedure and the physical models is presently being carried out under EPA Contract No. 68-02-1873. The UTRC method solves the axisymmetric time-averaged Navier-Stokes equations including the effects of turbulence, chemistry, radiation, and droplet vaporization. The FREP code has given reasonable predictions for combustor flow fields which have axial symmetry; however, significant circumferential asymmetry is present in many aircraft combustor flow fields and a realistic approach

- 
11. Gosman, A. D., W. M. Pun, A. K. Runchal, D. B. Spalding, and M. Wolfstein: Heat and Mass Transfer in Recirculating Flows. Academic Press, New York, (1969).
  12. Gosman, A. D. and W. M. Pun: Lecture notes for Course Entitled "Calculation of Recirculating Flows". Report No. HTS/7412, Department of Mechanical Engineering, Imperial College, London, (1974).
  13. Patankar, S. V. and D. B. Spalding: A Calculation Procedure for Heat, Mass and Momentum Transfer in Three-Dimensional Parabolic Flows. Int. J. Heat Mass Transfer, Vol. 15, p. 1787, (1972).
  14. Khalil, E. E., D. B. Spalding and J. H. Whitelaw: The Calculation of Local Flow Properties in Two-Dimensional Furnaces. Int. J. Heat Mass Transfer, Vol. 18, pp. 775-791, (1975).
  15. Gosman, A. D., F. C. Lockwood and S. A. Syed: Prediction of a Horizontal, Free, Turbulent Diffusion Flame. Proceedings Sixteenth Symposium (International) on Combustion, The Combustion Institute, (1976) to be published.
  16. Anasoulis, R. F., H. McDonald and R. C. Buggeln: Development of a Combustor Flow Analysis, Part I: Theoretical Studies. Air Force Aero Propulsion Laboratory Report AFAPL-TR-73-98, Part I, January 1974.

must consider this complication. Such a general approach involves solution of the time averaged three-dimensional Navier-Stokes equations including turbulence, chemical reactions, radiation transport and droplet vaporization. Recently, for instance, Patankar and Spalding (Refs. 17 and 18) have developed a line relaxation procedure for computation of steady three-dimensional combusting flows in cartesian or cylindrical polar geometries; however, this procedure is not generally available and few details of this technique have been disclosed at the present time.

Consequently, under Phase I of the present contract a three-dimensional combustor flow analysis program (Ref. 19) was developed by extending an existing and relatively efficient UTRC three-dimensional Navier-Stokes calculation procedure (Refs. 20 and 21) so that it would be able to compute combusting flows. In particular, the procedure developed included a simple mixing length turbulence model, a pseudo-kinetic hydrocarbon chemistry model, a liquid droplet vaporization model, a single frequency radiation model and a finite rate nitrogen oxide chemistry model.

The preliminary results obtained under Phase I for a rectangular combustion chamber demonstrated the feasibility of calculating three-dimensional time-dependent combusting flows using the MINT (Multidimensional Implicit Nonlinear Time-dependent) procedure. Experience from the Phase I study and from the two-dimensional EPA sponsored FREP program pointed out the severe shortcomings of the mixing length turbulence model due to the considerable difficulty in specifying a reasonable mixing length distribution even for relatively simple combustors. In addition the problem of significant truncation error because of the relatively coarse computational mesh (17 x

- 
17. Patankar, S. V. and D. B. Spalding: A Computer Model for Three-Dimensional Flow in Furnaces. Proceedings Fourteenth Symposium (International) on Combustion, The Combustion Institute, pp. 606-614, (1973).
  18. Patankar, S. V. and D. B. Spalding: Simultaneous Predictions of Flow Pattern and Radiation for Three-Dimensional Flames. Heat Transfer in Flames, Edited by N. Afgan and J. Beer. Scripta, Washington, (1974).
  19. Gibeling, H. J., H. McDonald and W. R. Briley: Development of a Three-Dimensional Combustor Flow Analysis, Vol. I: Theoretical Studies. Air Force Aero-Propulsion Laboratory Report AFAPL-TR-75-59, Vol. I, July 1975.
  20. Briley, W. R. and H. McDonald: An Implicit Numerical Method for the Multidimensional Compressible Navier-Stokes Equations. United Aircraft Research Laboratories Report M911363-6, November 1973.
  21. Briley, W. R., H. McDonald and H. J. Gibeling: Solution of the Multidimensional Compressible Navier-Stokes Equations by a Generalized Implicit Method. United Technologies Research Center Report R75-911363-15, January 1976.

9 x 17 grid) which was employed became apparent during Phase I of this program. In three-dimensional combusting flow calculations at present the computer run times are still too long to permit increasing the number of mesh points significantly to attain the desired accuracy. The Phase I results also indicated the need for a practical finite-rate chemistry model for premixed aircraft-fuel and air mixtures which could be incorporated into an elliptic computational procedure such as MINT. The latter problem is one of considerable complexity, and it seemed appropriate to defer work in this area until a future study.

Therefore, the Phase II effort under the present contract was directed toward incorporation of both a two-equation turbulence model and certain approximate nonlinear difference formulas into the MINT combustion code. The so-called nonlinear difference formulas represent an ad hoc adaptation of five-point central difference formulas into the three-point implicit difference framework of the MINT code, in order to alleviate the problem of truncation error associated with coarse computational grids. While the various formulas considered gave acceptable results in nonreacting flows, unfortunately no convergent solutions with the nonlinear formulas were obtained for combusting flows. Therefore, the numerical predictions presented herein were obtained using conventional central difference formulas. As a consequence of being unable to refine the computational grid due to computer run time limitations, the resulting combusting flow calculations with conventional central difference formulas almost certainly contain significant truncation errors, thus comparisons with experiment can only be viewed qualitatively. In addition, the inlet conditions for the experiment are known only approximately, further confusing the comparison between predictions and measurement. On the positive side, it was possible to perform stable calculations for a very complex reacting flow using a two-equation model of turbulence. The principle obstacle to a thorough evaluation of the procedure is simply insufficient grid points together with insufficient data on inlet conditions. The increased storage requirements of the additional grid points required to define the flow field accurately do not pose a particular problem in view of the efficient use of mass storage possible with the MINT code.

## SECTION II

### TURBULENCE MODEL

#### Turbulence Model Equations

The flow in combustion devices is known to be predominately turbulent. To account for this turbulent behavior in the solution of the time-average Navier-Stokes equations, a turbulence model is introduced to define an effective viscosity. A review of turbulence models is available in the literature (e.g. Refs. 22 to 24). Prandtl (Ref. 25) was perhaps the first to introduce a turbulence model when he postulated that the time-averaged shear stress and the time-averaged velocity gradient are proportional as in laminar flow, and that the length scale (the so-called mixing length) which enters the relationship is proportional to the turbulent shear region thickness. Prandtl's mixing length model has been employed successfully by a number of investigators (e.g., Refs. 26 to 30) in a variety of problems primarily involving turbulent flow along walls and in free turbulent flows. A disadvantage of the mixing length model is that it is an equilibrium model (i.e., turbulence is assumed to be produced and dissipated locally) and it requires an ad hoc

- 
22. Launder, B. E. and D. B. Spalding: *Mathematical Models of Turbulence*. Academic Press, London, 1972.
  23. Harlow, F. H., ed.: *Turbulence Transport Modeling*. AIAA Selected Reprint Series, Vol. XIV, 1973.
  24. Launder, B. E.: *Progress in the Modeling of Turbulent Transport*. Notes for Course on Turbulent Recirculating Flows-Prediction and Measurement, Pennsylvania State University, July 1975.
  25. Prandtl, L.: *Bericht Uber Untersuchungen Zur Ausgebildeten Turbulenz*. ZAMM, Vol. 5, 1925, p. 136.
  26. Patankar, S. V. and D. B. Spalding: *Heat and Mass Transfer in Boundary Layers*. Intertext Books, London, 1970.
  27. Maise, G. and H. McDonald: *Mixing Length and Kinematic Eddy Viscosity in a Compressible Boundary Layer*. AIAA Journal, Vol. 6, 1968, pp. 73-80.
  28. McDonald, H. and F. J. Camarata: *An Extended Mixing Length Approach for Computing the Turbulent Boundary Layer Development*. Proceedings of the AFOSR-IFP-Stanford Conference on Boundary Layer Prediction, 1968.
  29. Williamson, J. W.: *An Extension of Prandtl's Mixing Length Theory*. Applied Mechanics and Fluids Engineering Conference, ASME, June 1969.
  30. Lilley, D. G.: *Prediction of Inert Turbulent Swirl Flows*. AIAA Paper No. 72-699, 1972.

mixing length distribution. Some of the shortcomings of the mixing length model have been overcome for many cases of interest by the introduction of various multiequation transport models of turbulence.

Many of the two-equation turbulence models employ the Prandtl-Kolmogorov formula for specification of the turbulent viscosity,  $\mu_T$ ,

$$\frac{\mu_T}{\text{Re}} = C_\mu' \rho k^{1/2} \ell \quad (1)$$

where  $k$  is the turbulence kinetic energy and  $\ell$  is a length scale of the turbulence. This relation follows from dimensional arguments for turbulent flow described by the two parameters,  $k$  and  $\ell$ . A major advantage of a two-equation turbulence model compared to a mixing length model is the fact that the length scale (as well as the turbulence kinetic energy) is determined from transport equations, whereas in mixing length models the length scale is determined from an ad hoc algebraic expression. Successful use of the mixing length model requires an a priori specification of the turbulence length scale. While a realistic assumption can be made for certain flows such as shear layers, in many flows of interest (such as internal recirculating flows) the choice of a proper turbulence length scale is not obvious. Since the turbulence length scale emerges from the solution in a two-equation model, these models are more likely to give accurate predictions over a wide range of geometric and flow conditions with the same empirical constants.

It should be noted that the two equation models employ the eddy-viscosity formulation for the Reynolds stresses as in the mixing length model, i.e.,

$$\rho \overline{u_i' u_j'} = - \frac{\mu_T}{\text{Re}} \frac{\partial u_j}{\partial x_i} \quad (2)$$

Hence, this formulation still suffers from the physical shortcoming that there is zero Reynolds stress wherever the velocity gradient is zero. In addition, the eddy viscosity formulation is isotropic which may be incorrect in many three-dimensional and swirling flows. However, for practical calculations of turbulent internal recirculating flows there are no other available transport models which are as suitable or even as relatively well developed. In the present MINT computer code there are three mixing length models and one two-equation transport model of turbulence. Each mixing length model can be used individually or criteria can be specified such that the appropriate mixing length model will be utilized in various regions of the flow field. These models will now be discussed in some detail.

The mixing length turbulence models employed in this analysis are based on mixing length distributions suggested by Williamson (Ref. 29), Lilley (Ref. 30), and van Driest (Ref. 31). Williamson's model is applicable to flows in channels and pipes. Lilley's model is applicable to unconfined jet flows, and the van Driest model is valid for flows near solid walls. The mathematical form of the expression for the turbulent viscosity follows from Ref. 32:

$$\frac{\mu_T}{\text{Re}} = \rho \ell^2 (2\bar{\bar{e}}:\bar{\bar{e}})^{1/2} \quad (3)$$

where  $\bar{\bar{e}}$  is the mean flow rate of strain tensor

$$\bar{\bar{e}} = 1/2 [(\nabla\vec{u}) + (\nabla\vec{u})^T] \quad (4)$$

and the mixing length  $\ell$  is given by either Williamson's model

$$\frac{\ell}{r_0} = 0.14 \left(\frac{y}{r_0}\right) \exp\left(1 - \frac{y}{r_0}\right) \quad (5)$$

or Lilley's model

$$\frac{\ell}{r_0} = 0.08 \left(\frac{\Delta}{r_0}\right) \frac{w}{w_{\max}} = 0.05 \quad (6)$$

or van Driest's model

$$\ell = \kappa y \left[1 - \exp(-y/A^*)\right] \quad (7)$$

In the above expressions for  $\ell$ ,  $r_0$  is the distance from the wall to the centerline of the duct or pipe,  $y$  is the distance from the point in question to the nearest wall,  $\Delta$  is the half-width of a shear-layer like region as defined by Eq. (6) and  $\kappa$  and  $A^*$  are the von Kármán constant and van Driest damping coefficient, respectively. The constants in Eqs. (5-7) have been determined by comparison of theory and experimental data for the class of flows under consideration.

- 
31. van Driest, E. R.: On Turbulent Flow Near a Wall. Journal of the Aeronautical Sciences, November 1956.  
 32. Beer, J. M. and N. A. Chigier: Combustion Aerodynamics. Wiley, New York, 1972.

Various forms of the two equation model of turbulence have been proposed since Kolmogorov (Ref. 33) first introduced the concept in 1942. Most investigators have chosen the kinetic energy of turbulence,  $k$ , as their first variable. However, there is a wide diversity of choice as to the second variable to be used. In general, each investigator chose a second variable which he felt was appropriate to the physical description of turbulence. For instance, Kolmogorov chose as his second variable a quantity which was proportional to the mean frequency of the most energetic motions, while Spalding (Ref. 34) and Saffman (Ref. 35) chose a quantity that represented the time-average square of the vorticity fluctuations. Another commonly chosen second variable has been the turbulence kinetic energy dissipation rate,  $\epsilon$ , which was selected for this investigation. An advantage of using the dissipation rate of turbulence kinetic energy for the second equation is that the dissipation rate appears directly in the turbulence kinetic energy equation, and that an equation for  $\epsilon$  can be readily developed. Since derivation of the equations for  $k$  and  $\epsilon$  are lengthy and have previously been presented in the open literature, these derivations are not repeated in the present report. The appropriate transport equations for turbulence kinetic energy and energy dissipation rate valid at high Reynolds numbers are taken directly from Launder and Spalding (Ref. 36).

The turbulence kinetic energy equation in vector notation is

$$\frac{\partial(\rho k)}{\partial t} = -\nabla \cdot (\rho \vec{u} k) + \frac{1}{Re} \nabla \cdot \left( \frac{\mu_T}{\sigma_k} \cdot \nabla k \right) + \frac{\mu_T}{Re} (2\vec{\bar{e}} : \vec{\bar{e}}) - \rho \epsilon \quad (8)$$

where the first two terms on the right hand side represent convection and diffusion of turbulence kinetic energy, respectively; the third and fourth terms represent the generation (due to shear forces) and dissipation of turbulence kinetic energy, respectively. The equation for the dissipation rate of turbulence kinetic energy is

$$\frac{\partial(\rho \epsilon)}{\partial t} = -\nabla \cdot (\rho \vec{u} \epsilon) + \frac{1}{Re} \nabla \cdot \left( \frac{\mu_T}{\sigma_\epsilon} \cdot \nabla \epsilon \right) + C_1 \frac{\mu_T}{Re} \frac{\epsilon}{k} (2\vec{\bar{e}} : \vec{\bar{e}}) - C_2 \rho \frac{\epsilon^2}{k} \quad (9)$$

- 
33. Kolmogorov, A. N.: Equations of Turbulent Motion of an Incompressible Turbulent Fluid. IZC. Adak. Naut. SSR Ser. Phys. VI, No. 1-2, 56, 1942.
  34. Spalding, D. B.: The Prediction of Two-dimensional, Steady Turbulent Flows. Imperial College, Heat Transfer Section Report EF/TN/A/16, 1969.
  35. Saffman, P. G.: A Model for Inhomogenous Turbulent Flow. Proc. Roy. Soc. Ser. A317, 1970, p. 417.
  36. Launder, B. E. and D. B. Spalding: The Numerical Computation of Turbulent Flows. Computer Methods in Applied Mechanics and Engineering, Vol. 3, 1974, p. 269.

where the function of the terms is analagous to that in the turbulence kinetic energy equation. In Eqs. (8) and (9),  $\bar{\epsilon}$  is the mean flow rate of strain tensor defined by Eq. (4). Using dimensional arguments the Prandtl-Kolmogorov formula, Eq. (1) may be written as

$$\frac{\mu_T}{Re} = C_\mu \frac{\rho k^2}{\epsilon} \quad (10)$$

which implies a turbulence length scale or "mixing length" may be defined as

$$l = C_l \frac{k^{3/2}}{\epsilon} \quad (11)$$

The constants appearing in Eqs. (8-10) have been evaluated by Jones and Launder (Ref. 37) and those values will be used in this work.

$$C_\mu = 0.09$$

$$C_1 = 1.55$$

$$C_2 = 2.0 \quad (12)$$

$$\sigma_k = 1.0$$

$$\sigma_\epsilon = 1.3$$

#### Boundary Conditions

Formulation of suitable boundary conditions to be employed with the  $k-\epsilon$  turbulence model has proven to be critical in recirculating flows. Launder and Spalding (Ref. 36) advocated setting the value of dissipation rate ( $\epsilon$ ) at one grid point away from the wall consistent with an analytic wall function formulation. The appropriate relation is obtained by considering the turbulence length scale in the near wall region.

The eddy viscosity mixing length model for  $\mu_T$  is

---

37. Jones, W. P. and B. E. Launder: The Prediction of Laminarization with a Two-equation Model of Turbulence. Int. J. Heat Mass Transfer, Vol. 15, 1972, p. 301.

$$\frac{\mu_T}{\text{Re}} = \rho \ell^2 (2\bar{\epsilon} \bar{\epsilon})^{1/2} \quad (13)$$

which is valid near a wall. The constant  $C_\ell$ , Eq. (11), may be evaluated by assuming turbulence equilibrium, i.e.,

$$\epsilon = \frac{\mu_T}{\rho \text{Re}} (2\bar{\epsilon} \bar{\epsilon}) = \ell^2 (2\bar{\epsilon} \bar{\epsilon})^{3/2} \quad (14)$$

Using Eq. (11) and the Prandtl-Kolmogorov formula yields

$$\frac{\mu_T}{\text{Re}} = \rho \ell^2 (2\bar{\epsilon} \bar{\epsilon})^{1/2} = C_\mu \frac{\rho k^2}{\epsilon} \quad (15)$$

so that one finally obtains

$$C_\ell = C_\mu^{3/4} \quad (16)$$

Then Eq. (11) provides a relation for  $\epsilon$  near a wall where the mixing length  $\ell$  is assumed to be known:

$$\epsilon = C_\mu^{3/4} \frac{k^{3/2}}{\ell} \quad (17)$$

The value of kinetic energy,  $k$ , at the first grid point away from the wall is obtained by solution of the  $k$ -transport equation, along with the approximate condition  $\delta^2 k / \delta n^2 = 0$  applied at that point.

Results from a two-dimensional study being performed under EPA sponsorship at UTRC have led to a revision in the wall function concepts described in Ref. 19. The modified wall function approach appears to be less restrictive than the method described in Ref. 19, and seems to give good results for a variety of flow configurations. The basic premise is that at one grid point away from the wall the normal derivatives of turbulent viscosity and velocity should be consistent with a wall function formulation. It can be shown from the analysis of van Driest (Ref. 31) that the general relations which are valid in the near wall region are

$$u^+ = u^+(y^+) \quad (18)$$

$$\frac{1}{\mu_T} \frac{\partial \mu_T}{\partial y} = \frac{1}{g(y, y^+)} \quad (19)$$

$$\left( \frac{\partial \tilde{u}}{\partial y} \right)^{-1} \left( \frac{\partial^2 \tilde{u}}{\partial y^2} \right) = - \left( 1 - \frac{\partial u^+}{\partial y^+} \right) \frac{1}{\mu_T} \frac{\partial \mu_T}{\partial y} \quad (20)$$

where  $\tilde{u}$  is the total velocity component parallel to the wall,  $\mu_T$  is the turbulent viscosity, and  $y$  is the distance from the wall. Also,  $y^+$  and  $u^+$  are defined in the conventional manner as

$$y^+ = y \left( \frac{\rho u^*}{\mu_{10m}} \right) \text{Re} \quad (21)$$

$$u^+ = \frac{\tilde{u}}{u^*} \quad (22)$$

and the friction velocity  $u^*$  is given by

$$u^* = \left( \frac{\tau_w}{\rho} \right)^{1/2} \quad (23)$$

The function  $g(y, y^+)$  in Eq. (19) varies from  $y/2$  in the laminar sublayer to  $y$  in the logarithmic region. The functional form for  $u^+$  implied by Eq. (18) could be obtained, for example, from the analysis of van Driest (Ref. 31) or from the more empirical relations given by Walz (Ref. 38). In the logarithmic velocity profile region ( $y^+ \gtrsim 60$ ), the conventional law of the wall can be written

$$u^+ = c_1 \ln y^+ + c_2 \quad (24)$$

and relations (19-20) reduce to

$$\frac{1}{\mu_T} \frac{\partial \mu_T}{\partial y} = - \left( \frac{\partial \tilde{u}}{\partial y} \right)^{-1} \left( \frac{\partial^2 \tilde{u}}{\partial y^2} \right) = \frac{1}{y} \quad (25)$$

These relations (25) serve to specify a wall value of turbulent viscosity and a wall "slip" velocity such that the normal derivatives are consistent with the logarithmic wall function formulation. Note that Eq. (25) is independent of the constants  $c_1$  and  $c_2$  appearing in Eq. (24), and hence this approach appears to be less restrictive than using Eq. (24) directly. These relations have been employed in the calculations carried out under Phase II of the present contract without difficulty, although flow resolution in the region very near the wall is sacrificed to attain accuracy in the central region of the flow field where the combustion processes are

---

38. Walz, A.: Boundary Layers of Flow and Temperature. M.I.T. Press, Cambridge, Massachusetts, p. 115, 1969.

concentrated. However, if accurate calculations in the wall region are required at a later date, refinements to the wall function approach may be implemented easily in the present computational procedure.

Another problem arising in the practical application of a two equation turbulence model which has not been widely discussed is the difficulty of specifying suitable function boundary conditions for  $k$  and  $\epsilon$  at a computational inlet plane. In modeling a general experimental configuration, the problem of specifying  $k$  and  $\epsilon$  at the inlet plane is complicated by the lack of detailed inlet velocity and turbulence profiles. Hence, it is necessary to assume the inlet velocity profile and then construct consistent profiles for  $k$  and  $\epsilon$  therefrom. In general one possibility is to assume turbulence equilibrium and a mixing length distribution, i.e., Eq. (14). Then using Eq. (10),

$$k = \frac{\ell^2 (2\bar{e} \cdot \bar{e})}{\sqrt{c_\mu}} \quad (26)$$

and  $\epsilon$  follows from Eq. (14). A difficulty with this approach occurs when the velocity profile becomes uniform, since the rate of strain tensor ( $\bar{e}$ ) approaches zero. It is known that a "free stream" turbulence level exists in virtually all uniform flows, suggesting that a specified free stream turbulence kinetic energy,  $k_{FS}$  be added to Eq. (26) to provide the total inlet turbulence level,

$$k = k_{FS} + \frac{\ell^2 (2\bar{e} \cdot \bar{e})}{\sqrt{c_\mu}} \quad (27)$$

where  $\ell$  is still the specified mixing length. The addition of free stream turbulence implies that equilibrium no longer exists in general, and  $\epsilon$  follows from Eq. (17). The addition of free stream turbulence as indicated in the above procedure seems to provide reasonable values for the turbulence variables  $k$ ,  $\epsilon$  and  $\mu_T$ ; and the resulting solutions exhibit qualitatively reasonable behavior.

#### Numerical Considerations

Efficient solution of the  $k$ - $\epsilon$  model governing equations, Eqs. (8-10), together with the conservation equations of mass, momentum, energy and species described in Ref. 19 requires proper treatment of the source terms in Eqs. (3) and (9). The calculation procedure of Ref. 19 employed a mixing

length turbulence model and an eddy viscosity evaluated from the known solution at time level  $t^n$ . This procedure has also been used with the k- $\epsilon$  turbulence model, Eqs. (8-10). The source terms in Eqs. (8-9) may then be linearized in accordance with the technique discussed in Refs. (19 to 21). Of course, it is then necessary to solve the k- $\epsilon$  equations in a coupled manner. However, since k and  $\epsilon$  serve only to specify the turbulent viscosity through Eq. (10), it is in fact possible to solve the k- $\epsilon$  finite difference equations after determination of the flow field for a given time step. This approach requires considerably less computer run time than the alternate procedure of solving the complete system of algebraic equations in a coupled fashion, and has been employed successfully in computing the results contained in this report.

### SECTION III

#### SPATIAL DIFFERENCE FORMULATION

In computing solutions for high Reynolds numbers with a conventional centered second order accurate spatial derivative, it is often found necessary to add a form of artificial viscosity or dissipation for the axial flow direction. Artificial dissipation in some form is often useful in practical calculations to stabilize the overall method when boundary conditions are treated inaccurately, when coarse mesh spacing is used, or in the presence of discontinuities. The need for artificial dissipation arises in certain instances when centered spatial difference approximations are used for first derivative terms. The use of artificial dissipation is thus a matter of spatial differencing technique, and is commonly employed either explicitly or implicitly in both explicit and implicit difference schemes. The main problem with artificial dissipation encountered in the present work is the resultant smearing of the solution which occurs in a high Reynolds number flow with inadequate mesh resolution. The particular form of artificial diffusion described here is considered provisional, since the formal accuracy is lowered to first order for the axial ( $x_3$ ) coordinate direction. Another combination of spatial difference formulas and/or artificial viscosity terms may eventually prove superior. The objective of this phase of the present work was to investigate and utilize a spatial difference formulation which would yield stable solutions with reduced numerical smearing. A preliminary evaluation of an alternative first derivative formula which had some potential to eliminate the artificial viscosity was made, and this alternate difference scheme will be discussed subsequently.

The dissipation term used here for the conventional second order accurate first-derivative is based on an observation (Roach, Ref. 39, p. 162) that for a linear model problem representing a one-dimensional balance of convection and diffusion terms,

$$u_i \frac{\partial \phi}{\partial x_i} = \frac{1}{\text{Re}} \frac{\partial^2 \phi}{\partial x_i^2} \quad (28)$$

---

39. Roache, P. J.: Computational Fluid Dynamics. Hermosa Publishers, Albuquerque, 1972.

it can be shown by a comparison with an exact solution of Eq. (28), solutions obtained using central differences for the convection term are well behaved provided the mesh Reynolds number  $Re_{\Delta x_i} = |u_i| \Delta x_i Re$  is  $\leq 2$ , but that qualitative inaccuracies (associated with boundary conditions) may occur when  $Re_{\Delta x_i} > 2$ . This suggests the use of an artificial viscosity to ensure that the local effective mesh Reynolds number is no greater than two. Thus, Eq. (28) is replaced by

$$u_i \delta_i \phi = \left( \frac{1}{Re} + \epsilon_i \right) \delta_i^2 \phi \quad (29)$$

where

$$\epsilon_i = \begin{cases} \frac{1}{Re} \left( \frac{Re_{\Delta x_i}}{2} - 1 \right) & \text{if } Re_{\Delta x_i} > 2 \\ 0 & \text{if } Re_{\Delta x_i} \leq 2 \end{cases} \quad (30)$$

From Eq. (30), it is apparent that the artificial viscosity can be made to vanish by refining the mesh. Since the artificial viscosity is proportional to  $\Delta x_i$ , solutions will have first-order formal accuracy if  $Re_{\Delta x_i} > 2$  but second-order accuracy if  $Re_{\Delta x_i} \leq 2$ . Strictly speaking, the overall method is second-order accurate since  $Re_{\Delta x_i} \rightarrow 0$  as the mesh is refined. It should be remembered, however, that such asymptotic truncation error estimates are meaningful only for sufficiently small mesh size; whereas, in practical calculations of complex flows, mesh resolution capabilities have often, out of necessity, been strained. One virtue of the present formulation is that by isolating the artificial viscosity terms for comparison with other terms in the equations, a nonrigorous but plausible a posteriori indication of the first order truncation error in a computed solution is available. It is, of course, obvious that Eq. (29), upon which the artificial viscosity is based, represents a gross simplification of the Navier-Stokes equations, and it is primarily for this reason that the present formulation of artificial viscosity terms is considered provisional.

Particularly in the high Reynolds number type of three dimensional flows considered in the present work the number of grid points required to keep the cell Reynolds number less than two ( $Re_{\Delta x_i} \leq 2$ ) becomes prohibitive if less than multihour computer run times on a CDC 6600 are to be avoided. In many circumstances of interest in combusting flows, such as diffusion flames, the flow gradients and resulting physical diffusion are such that the use of an artificial viscosity or diffusion coefficient applied to such large gradients can seriously degrade the solution by the introduction of significant artificial numerical diffusion. Various strategies have been

and are being evolved to circumvent this difficulty. Of particular note is the revived interest (Orszag & Israeli, Ref. 40) in fourth-order compact difference formulas involving only three grid points. Mitchell (Ref. 41) for instance, cites some early applications of this technique within the ADI framework. Unfortunately these compact difference formulas lose a great deal of their attractiveness when both first and second derivatives in the same coordinate direction are present, since it turns out that the first and second derivatives each require a separate computational level within the ADI procedure. In terms of computational effort, Briley, McDonald and Gibeling (Ref. 21) estimated that the fourth order compact difference schemes required about the same amount of work as did the more conventional five point centered fourth order accurate difference formulas. The key point remains, however, that if Orszag and Israeli's (Ref. 40) estimate is valid of the possible reduction in the number of grid points for the fourth order schemes relative to the second order schemes to achieve comparable accuracy, very significant benefits are to be obtained from using higher order accurate schemes in multidimensional problems. It was not possible within the constraints of the present study to accomplish the necessary code modifications required to permit the enlargement of the finite difference molecule in the MINT code from three to five points. Nor was it possible to introduce the conventional compact three-point fourth order scheme without a significant effort in view of the additional levels required within the ADI framework. Instead a rather simple compact scheme which could be easily implemented into the present scheme was evaluated. This simple compact scheme will now be described.

The centered fourth order accurate five-point first derivative formula can be written for equally spaced mesh as

$$\frac{\partial \phi}{\partial x} = \frac{1}{2\Delta x} \left[ \phi_{i+1} - \phi_{i-1} - \frac{1}{6} (\phi_{i+2} - 2\phi_{i+1} + 2\phi_{i-1} - \phi_{i-2}) \right] + O(\Delta x^4) \quad (31)$$

Next it is assumed that between grid points the function  $\phi$  can be represented by some exponential. It then follows that

$$\phi_{i+2} = \phi_{i+1}^2 / \phi_i, \quad \phi_{i-2} = \phi_{i-1}^2 / \phi_i \quad (32)$$

---

40. Orszag, S. A. and M. Israeli: Numerical Simulation of Viscous Incompressible Flows. Annual Reviews in Fluid Mechanics, Vol. 6, 1974, p. 281.

41. Mitchell, A. R.: Computational Methods in Partial Differential Equations, Wiley, New York, 1969.

thus allowing the five point difference molecule to be compressed to three, which after a little manipulation gives

$$\frac{\partial \phi}{\partial x} \approx \frac{\phi_{i+1} - \phi_{i-1}}{2\Delta x} \left[ 1 - \frac{\phi_{i+1} - 2\phi_i + \phi_{i-1}}{6\phi_i} \right] \quad (33)$$

$$= \delta \phi_i \left[ 1 - \Delta x^2 \delta^2 \phi_i / 6\phi_i \right] \quad (34)$$

Now it is easily verified that on linear combinations of sine, cosine and exponential functions the given formula is fourth order accurate. It is also apparent that the formula is nonlinear and must encounter difficulties as  $\phi_i$  passes through zero. Further although the formula as given is not independent of a translation by a constant in the dependent variable  $\phi_i$ , translation by an additive constant would eliminate the zero denominator problem. If this additive constant were infinite the conventional three point second order central difference formula for the first derivative is recovered, and as mentioned earlier if the additive constant were zero a fourth order accurate formula for sines, cosines and exponentials, not suffering a cell Reynolds number of two limitation, is recovered. Under this effort an ad hoc limit was placed upon the correction term  $\Delta x^2 \delta^2 \phi_i / 6\phi_i$ ; this term was limited to a value of 0.5. This procedure avoids the difficulty associated with a zero denominator. Insofar as the nonlinear aspect of the formulation is concerned this was readily treated using the time linearization concept (Refs. 19 to 21) previously introduced to treat the nonlinear dependent variable terms in the governing equations. For ease of implementation the denominator term was not linearized but treated explicitly. This was felt reasonable for a preliminary evaluation, since if warranted by the results this explicit term could be treated more precisely at the expense of some tedium.

Under the present effort the nonlinear difference formula was applied to the continuity equation for a simple axisymmetric diffusion flame in a cylindrical pipe in which there was no reverse flow. The result of this application was a reduction of the mass flux error at the computational exit plane from about thirteen (13) percent to less than one percent. Finally the scheme was applied to the three-dimensional rectangular combustor discussed in Section IV, but a convergent solution could not be obtained. The source of the numerical difficulty was felt to be related to the still too coarse mesh and to the form of the first-derivative correction term in Eq. (34), i.e.,  $(\Delta x)^2 \delta^2 \phi_i / 6\phi_i$ . The correction term can give a major contribution to the derivative in regions with large second derivatives of the dependent variables, particularly when the variable  $\phi_i$  is near zero, and this may lead

to erroneous results. Finally, the one-sided continuity equation wall boundary condition is difficult to formulate consistent with the nonlinear scheme Eq. (34), and this also may have contributed to the numerical problem. Within the constraints of the present program these difficulties could not be resolved. At this point the origin of the difficulties has not been established precisely so it is not even clear if the above scheme could be made to work satisfactorily for reacting flows with recirculation. Certainly the motivation to continue efforts to increase the accuracy and minimize the number of grid points for three-dimensional combusting flow calculations is still present.

## SECTION IV

### RESULTS AND CONCLUSIONS

To evaluate the three-dimensional computational procedure described in the previous sections, comparisons were made between numerical predictions obtained from the MINT code and unpublished experimental data taken in a rectangular research combustor by the Pratt & Whitney Aircraft (P&WA) Combustion Group. The P&WA results consisted of temperature measurements taken with a shielded thermocouple probe and emission measurements (unburned hydrocarbons, nitric oxide, carbon monoxide, carbon dioxide) taken using gas sampling probes. No other flow measurements were available for comparison. The P&WA research combustor is a rectangular duct with a cross section 1.5 by 3.0 in. and an overall length of about 10.0 in. The flameholder employed for the measurements described herein was a steel plate (0.25 in. thick) containing an array of eight (8) holes as shown in Fig. 2. The holes are 0.397 in. in diameter with 0.75 in. between hole centers. The P&WA combustion experiment employed prevaporized Jet-A aircraft fuel which was premixed with a preheated air stream. The nominal fuel composition was 85.9 weight percent carbon and 14.1 weight percent hydrogen with a molecular weight of 160.0; therefore, the nominal chemical formula for the fuel is  $C_{11.44}H_{22.38}$ . The fuel heat of combustion is approximately  $4.3 \times 10^7$  joule/kg (18500 Btu/lbm), and a constant fuel specific heat ( $c_p$ ) of 2510.0 joule/kg- $^{\circ}K$  (0.6 Btu/lbm- $^{\circ}R$ ) was used in the present calculations. The air preheat temperature measured far upstream of the flame holder was about 756 $^{\circ}K$  (900 $^{\circ}F$ ); the total mass flow rate through the combustor was  $2.86 \times 10^{-2}$  kg/sec; and the fuel mass fraction was 0.0322.

Unfortunately, subsequent thermocouple measurements in the P&WA combustor have shown the mixture temperature directly upstream of the flameholder to be approximately 1030 $^{\circ}K$  (1400 $^{\circ}F$ ). The higher temperature of 1030 $^{\circ}K$  believed to be present upstream of the flameholder may be attributed to heat transfer through the flameholder from the combustion zone to the gas mixture upstream of the flameholder, and possibly to fuel pyrolysis upstream of the flameholder. The downstream equilibrium temperature results obtained previously (Ref. 19) with an inlet temperature of 750 $^{\circ}K$  and adiabatic wall conditions indicate that there are significant energy losses in the combustor. Proper treatment of the flameholder boundary conditions would require additional information regarding the heat transfer or surface temperature of the flameholder. If there are significant energy losses through the flameholder, these would not be correctly represented by the adiabatic wall conditions actually employed in the calculations. However, correct incorporation of the heat transfer mechanism would be sensitive to the local gas temperature, and therefore, would require a reasonable representation of the hydrocarbon

combustion kinetics. For complex fuels such as Jet-A this is an extremely complicated problem, since the actual fuel pyrolysis mechanism is generally not known. Typically, one would be forced to assume a global partial oxidation reaction with CO and H<sub>2</sub> as products. Then a detailed reaction mechanism for oxidation of CO and H<sub>2</sub> to form the final products CO<sub>2</sub> and H<sub>2</sub>O could be employed. It should be apparent that even such a relatively "simple" approach to the combustion chemistry is still prohibitive in the context of a elliptic fluid mechanics calculation procedure, although some recent progress has been made in two-dimensional modeling of a well-stirred reactor by Wormeck and Pratt (Ref. 42).

The computational region boundaries considered in the present calculations are indicated by dashed lines in Fig. 2. In order to reduce the number of grid points required in the calculation the hole pattern was assumed to be periodic in the longitudinal direction, so that symmetry boundary conditions could be applied and only one-half of the inlet port need be considered, as shown in Fig. 2. The temperature measurements in the combustor indicate that this is a reasonable approximation. The computational region and coordinate system are illustrated in Fig. 3. Figure 4 shows the sections (A, B, C) for which profile plots of axial velocity, temperature, and nitric oxide are presented. All predictions presented were made using a 17 by 9 by 17 grid (2601 grid points) for the x<sub>1</sub>, x<sub>2</sub>, x<sub>3</sub> directions, respectively. A maximum axial velocity (U<sub>D</sub>) of 159.5 m/sec was required to match the experimental mass flow rate. The reference length (L) for all coordinates is 0.010905 meters (0.75 in.). The calculation was initiated downstream of the flameholder assuming a mixture inlet temperature of 1025°K and a pressure of 1.002 x 10<sup>5</sup> Pascals (atmospheric pressure). A somewhat arbitrary but plausible free stream turbulence kinetic energy level of ten percent (i.e., k<sub>FS</sub> = 0.1 U<sub>D</sub><sup>2</sup>/2) was imposed at the computational inlet plane.

Axial velocity profiles are given in Figs. 5, 6 and 7 at sections A, B, and C, respectively, for a series of axial stations. A series of cross-sectional plane contour plots of constant axial velocity are shown in Figs. 8 to 11 for various axial stations. The qualitative characteristics of the jet expanding into the combustor seem to be represented quite reasonably. As one proceeds away from the inlet, the jet spreading is evident and reverse flow is clearly present downstream of the flameholder wall region. Due to the large inlet velocity and the relatively small number of grid points employed in the calculation, cell Reynolds numbers in the axial direction became large

---

42. Wormeck, J. J. and D. T. Pratt: Computer Modeling of Combustion in a Longwell Jet-Stirred Reactor. Proceedings Sixteenth Symposium (International) on Combustion, The Combustion Institute, 1976, to be published.

so that significant artificial viscosity was required in the difference equations (see Section III). The presence of artificial viscosity in the present case resulted in a very unfortunate 17 percent increase in mass flux between the inlet and computational exit plane ( $x_3 = 4.0$ , nondimensional), due to the artificial diffusion term required in the continuity equation. Profiles of the calculated turbulence kinetic energy in the combustor are shown in Figs. 12, 13 and 14. The influence of the assumed inlet free stream turbulence level ( $k_{FS}$ ) seems to persist fairly far downstream of the inlet. The effect of  $k_{FS}$  variations on the pertinent solution variables was not investigated in the present study, but this question clearly needs to be addressed in future experimental and theoretical studies.

The equilibrium hydrocarbon chemistry assumption was not expected to be valid near the inlet port of the combustor under consideration. Therefore, an ad hoc ignition delay criterion was imposed on the solution to prevent unrealistically large temperature gradients from occurring near the inlet. This was accomplished in the present numerical procedure by specifying the pseudo-kinetic rate constant,  $k_{HC}$  (Ref. 19), as a function of axial distance from the inlet plane. The effect of the specified ignition delay on the port-centerline axial temperature variations is shown in Fig. 15, along with experimental measurements at four axial stations. As expected the predicted temperatures are considerably higher than the measured values because of the energy losses in the combustor which were not included in the calculations. Nondimensional temperature profiles are presented in Figs. 16 to 18 at sections A, B, and C, respectively, for a series of axial stations, and a sequence of cross-sectional plane contour plots of constant temperature are shown in Figs. 19 to 21. The available experimental temperature measurements are also displayed on Fig. 17 for section B. The presence of artificial viscosity (in the axial direction) in both the species and energy equations may have distorted the transverse temperature profiles, since outside the jet boundaries artificial diffusion is significant compared to convection. However, the qualitative comparisons which can be made from Fig. 17 indicate a reasonable variation of predicted temperature across the combustor. Only a limited number of nitric oxide (NO) concentration measurements were made in the combustor under consideration. Since the NO concentration is sensitive to the temperature history of a fluid particle, comparisons between prediction and experiment are not meaningful in this instance. The NO concentration profiles (Fig. 22) are shown only for the axial station where an equilibrium temperature has been achieved.

The present numerical results demonstrate both the basic integrity of the computational procedure developed under the present study and the capability of the MINT code to perform calculations of three-dimensional combusting flows with recirculation. The need for improvement of the differencing scheme is apparent because of the suspected distortion in the predictions due to excessive artificial viscosity. The preliminary efforts to develop a simple compact differencing scheme made under the present program showed some success in nonreacting flows, however, no reasonable results could be obtained for combusting flows. The ad hoc nature of the compact difference scheme proposed in Section III is an undesirable feature, and it may preclude successful use of schemes such as these for general problems. The motivation for continued development of higher order solution procedures should still be high for the reasons mentioned in Section III.

In addition, there is clearly a need for an improved hydrocarbon chemistry model in the existing computer code if reasonably accurate quantitative predictions are desired. For a general three-dimensional elliptic computational procedure such as the MINT code, it is felt that a relatively simple finite-rate hydrocarbon chemistry model should be employed, in conjunction with a simple model for representation of the influence of turbulent concentration fluctuations, such as that employed by Hutchinson, Khalil and Whitelaw (Ref. 43).

- 
43. Hutchinson, P., E. E. Khalil and J. H. Whitelaw: The Calculation of Wall Heat Transfer Rate and Pollution Formation in Axisymmetric Furnaces. Presented at 4th Members Conference, International Flame Research Foundation, Ijmuiden, Holland, May 1976.

## SECTION V

### FREP COMPUTER CODE

The two-dimensional FREP (Field Relaxation Elliptic Procedure) computer code had been developed at United Technologies Research Center under both Air Force and Environmental Protection Agency sponsorship for the prediction of combusting flow fields. Presently, the FREP code is being further developed under EPA contract number 68-02-1873 and this code is deliverable to the Air Force under the present contract. The theoretical analysis for the FREP code, comparison of computed results with measurements, and the user's manual for the FREP computer program will be available as EPA reports.

In order to demonstrate the FREP computer code on the Wright-Patterson Air Force Base CDC 6600 a sample two-dimensional problem was run. The geometry considered was similar to that in the three-dimensional computation with each array of four holes replaced by a slit, and the end-walls were neglected. The inlet temperature was taken as  $756^{\circ}\text{K}$  ( $900^{\circ}\text{F}$ ) with all other conditions as described in Section IV. An arbitrary linear ignition delay criterion (from inlet to exit plane) was applied in conjunction with equilibrium hydrocarbon chemistry for this demonstration calculation. The computed axial velocity profiles at several axial stations are shown in Fig. 23; the plane of symmetry and the channel wall are located at  $X_1 = 0.0$  and  $X_1 = 1.0$ , respectively, while the inlet port is centered between these two boundaries. The qualitative behavior of these profiles seems reasonable, in view of the coarse computational mesh ( $17 \times 17$ ) employed in this calculation. Extensive evaluation of the FREP code is being carried out under EPA contract 68-02-1873.

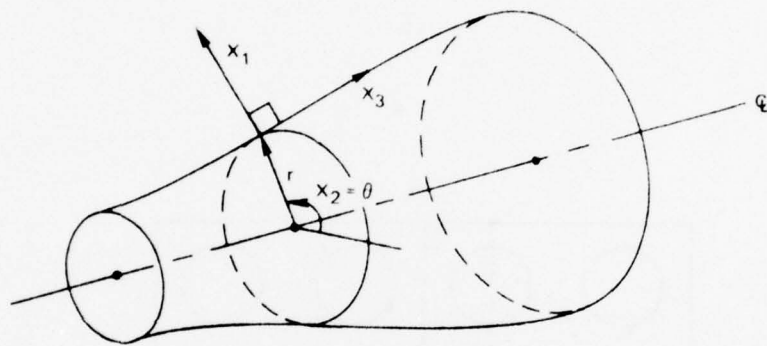
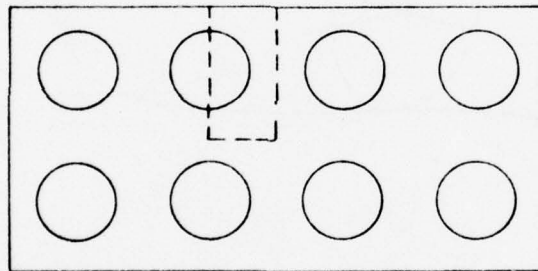


Figure 1. General axisymmetric combustor geometry.

NOTE: COMPUTATIONAL BOUNDARIES DENOTED BY DASHED LINES



**Figure 2. Experimental flameholder configuration for three dimensional rectangular combustor**

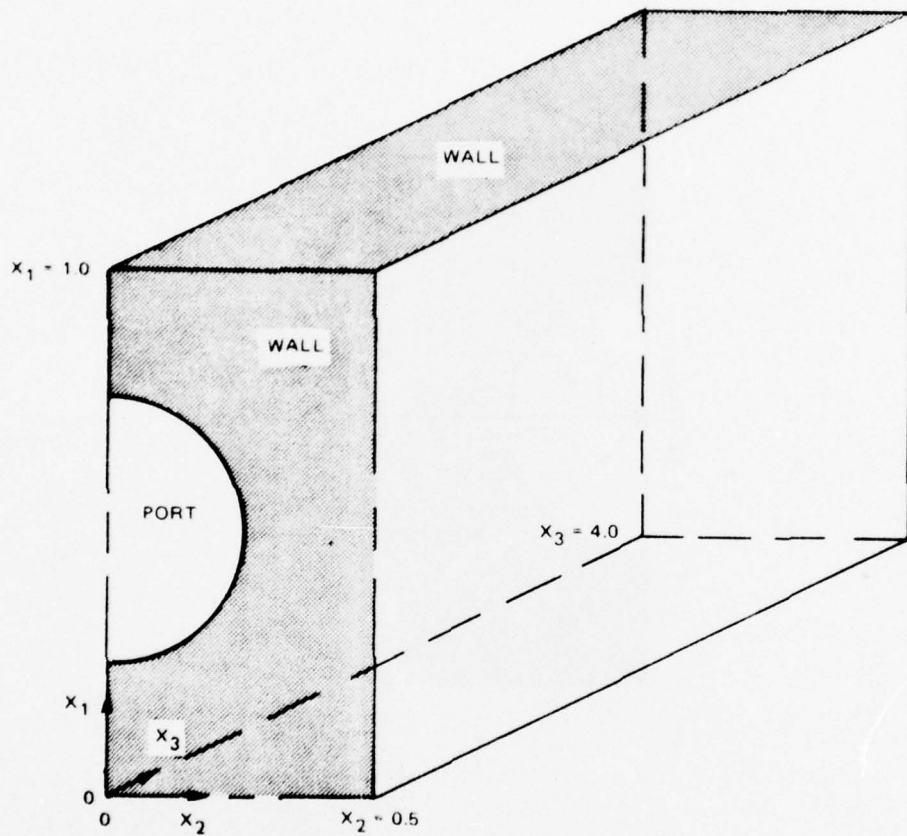


Figure 3. Computational region and coordinate system for three dimensional rectangular combustor

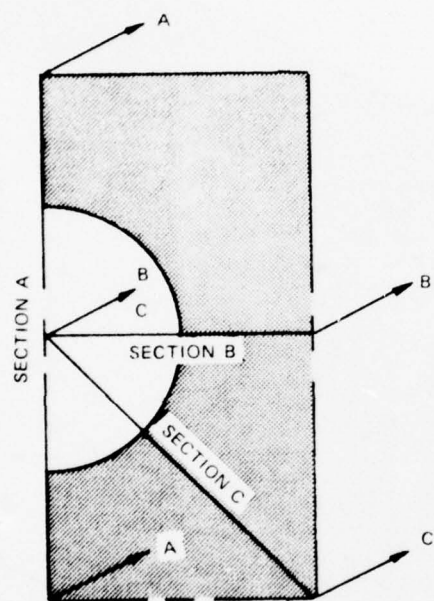


Figure 4. Cross flow plane sections A,B, and C for profile plots

SECTION A:  $x_2 = 0.0$

$U_D = 159.5 \text{ m/sec}$

$L = 0.01905 \text{ m}$

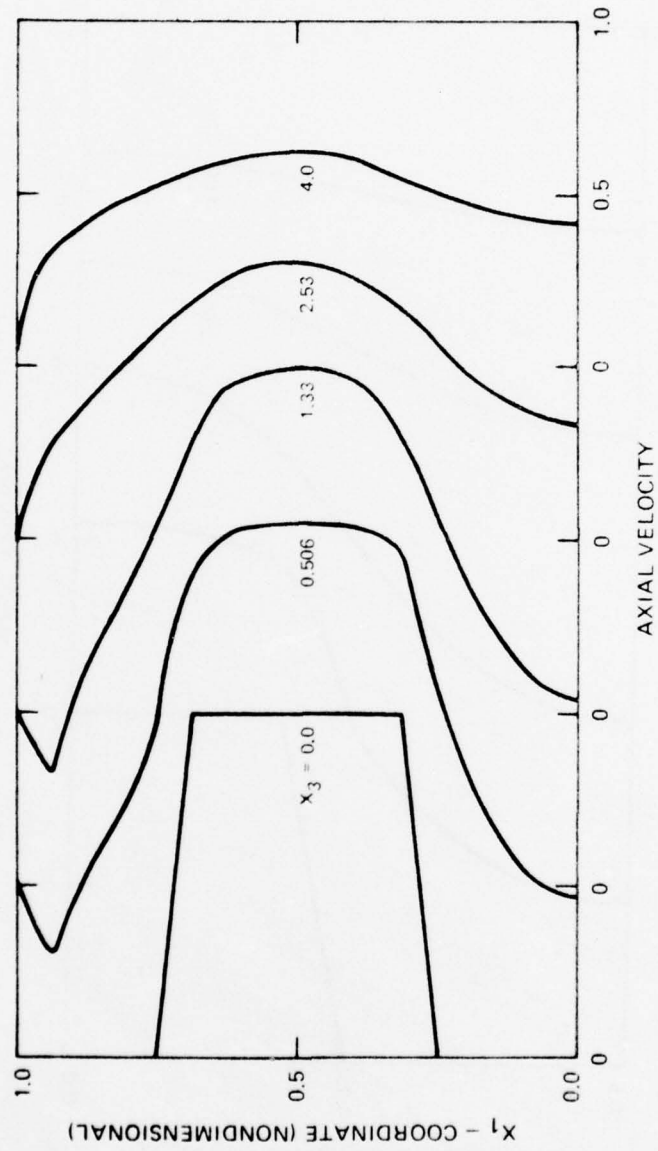


Figure 5. Nondimensional axial velocity profiles

SECTION B:  $X_1 = 0.5$

$U_D = 159.5$  m/sec

$L = 0.01905$  m

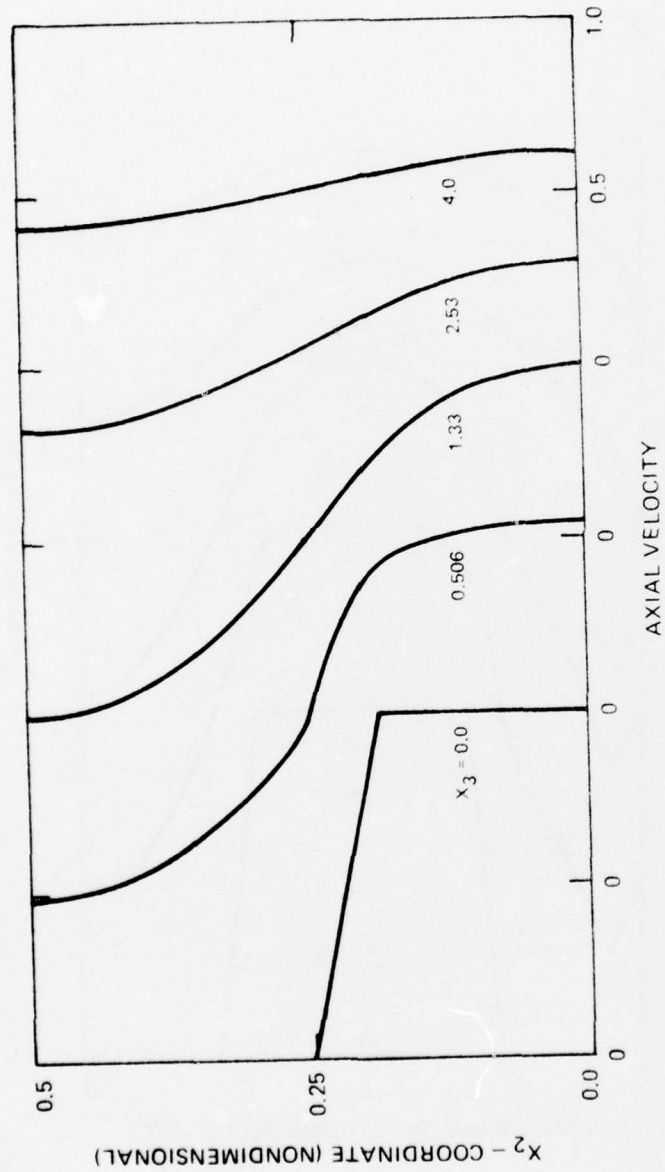


Figure 6. Nondimensional axial velocity profiles

SECTION C: DIAGONAL

$U_D = 159.5 \text{ m/sec}$

$L = 0.01905 \text{ m}$

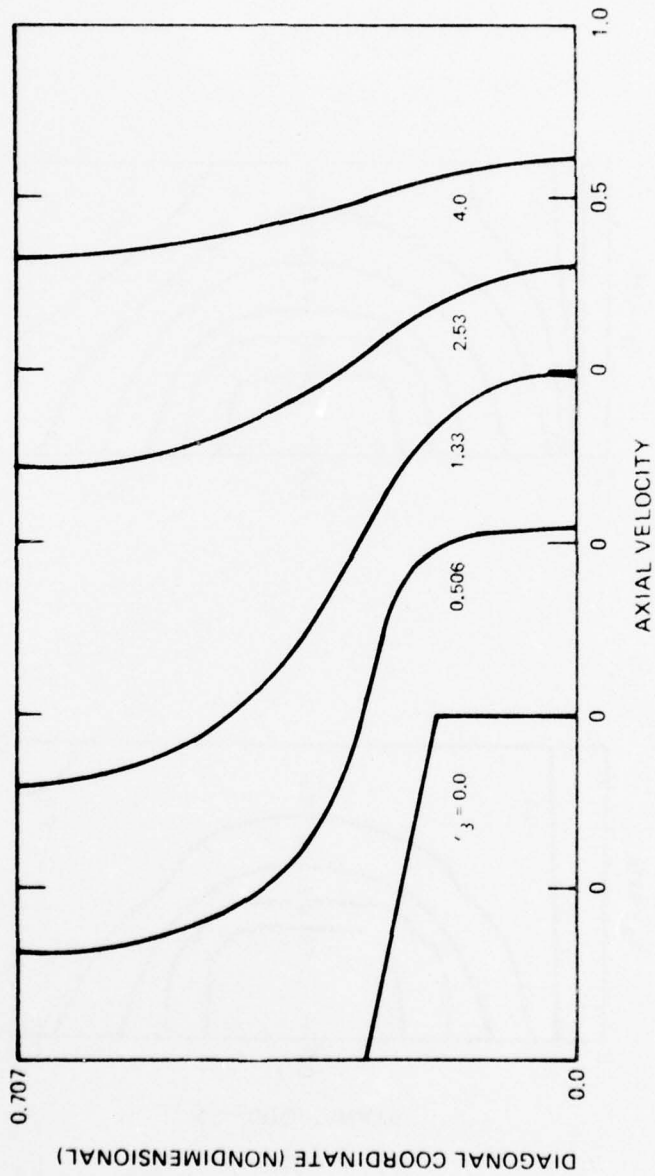


Figure 7. Nondimensional axial velocity profiles

$U_D = 159.5 \text{ m/sec}$   
 $L = 0.01905 \text{ m}$

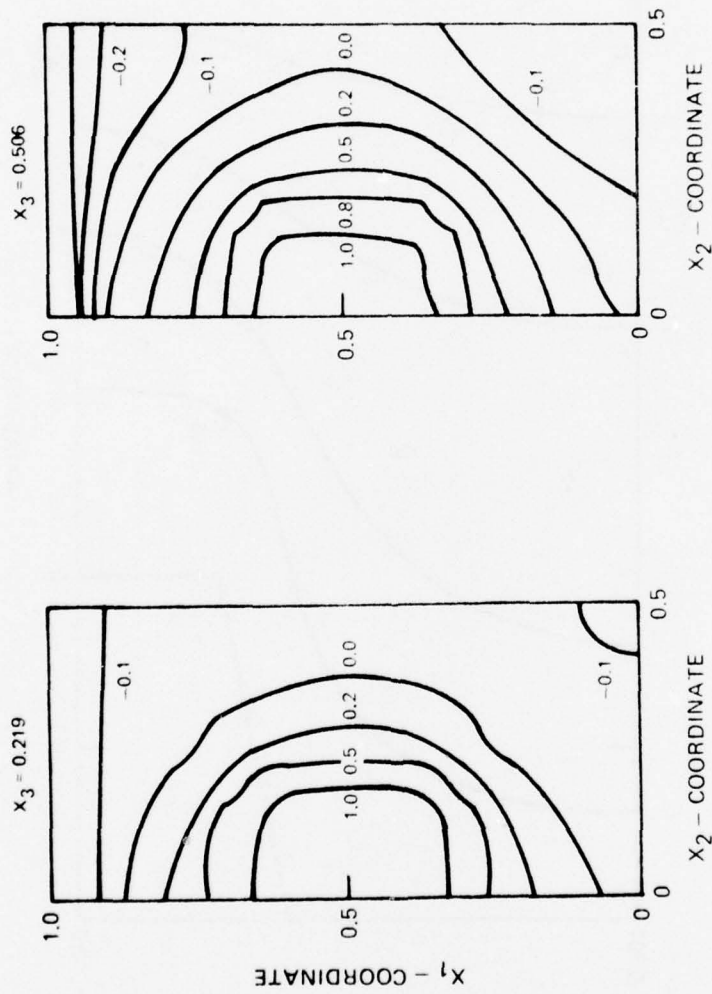


Figure 8. Contours of constant nondimensional axial velocity in the cross-sectional plane

$U_D = 159.5 \text{ m/sec}$   
 $L = 0.01095\text{m}$

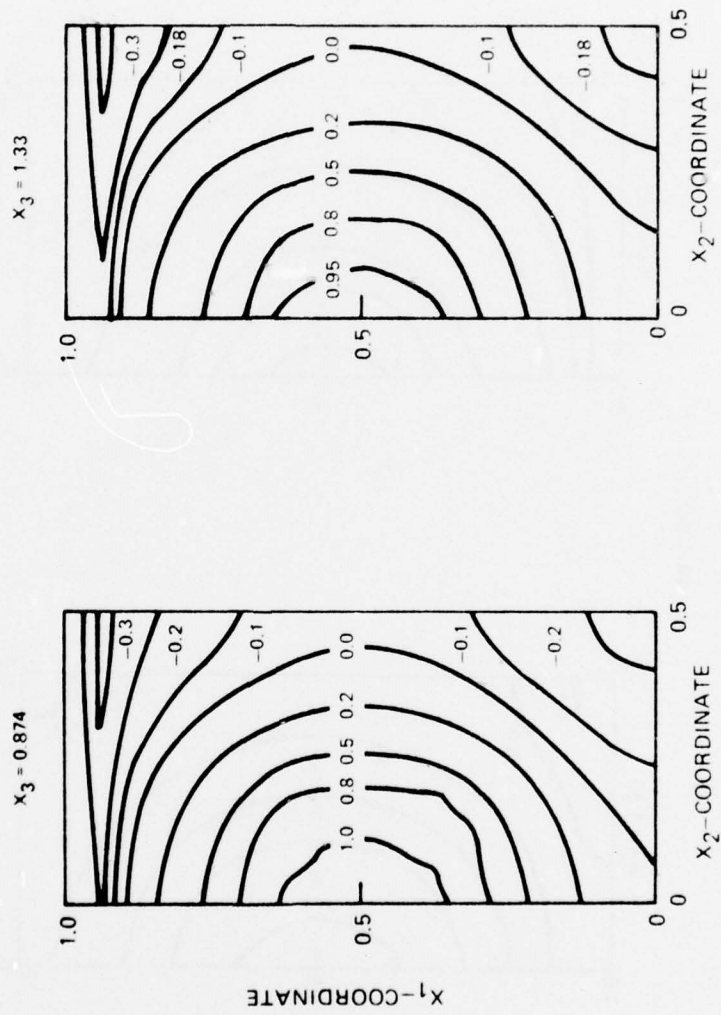


Figure 9. Contours of constant nondimensional axial velocity in the cross-sectional plane

$U_D = 159.5 \text{ m/sec}$   
 $L = 0.01905 \text{ m}$

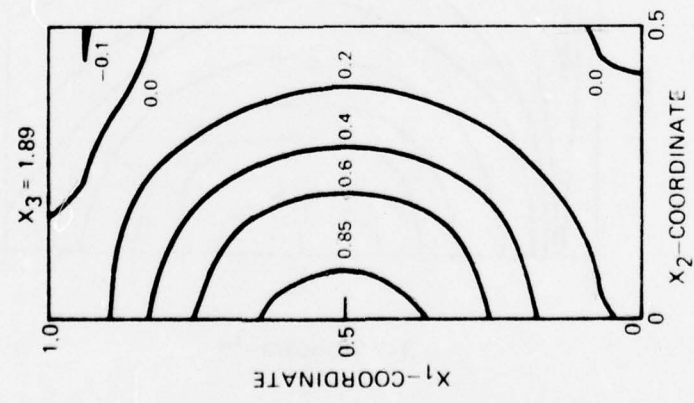
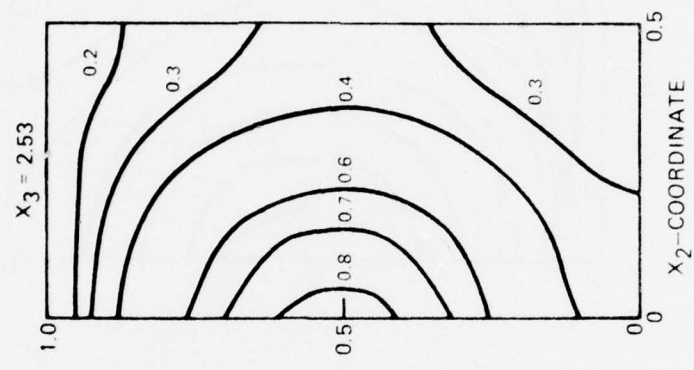


Figure 10. Contours of constant nondimensional axial velocity in the cross-sectional plane

$U_D = 159.5 \text{ m/sec}$

$L = 0.01905 \text{ m}$

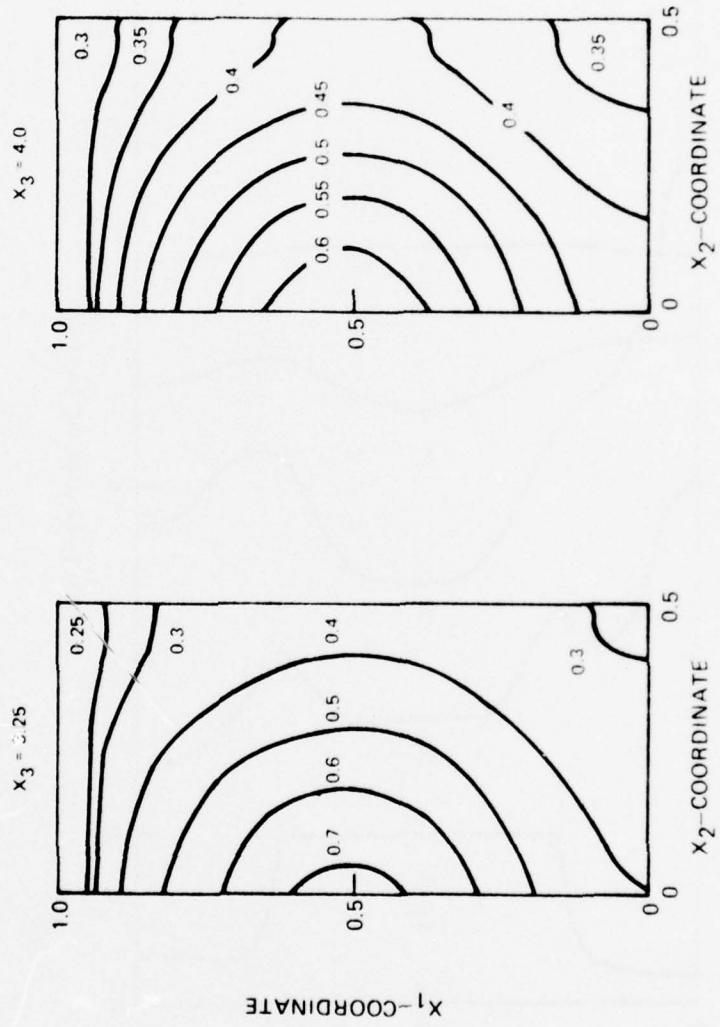


Figure 11. Contours of constant nondimensional axial velocity in the cross-sectional plane

SECTION A  $x_2 = 0.0$   
 $k_D = 2.544 \times 10^4 \text{ m}^2/\text{s}^2$   
 $L = 0.01905 \text{ m}$

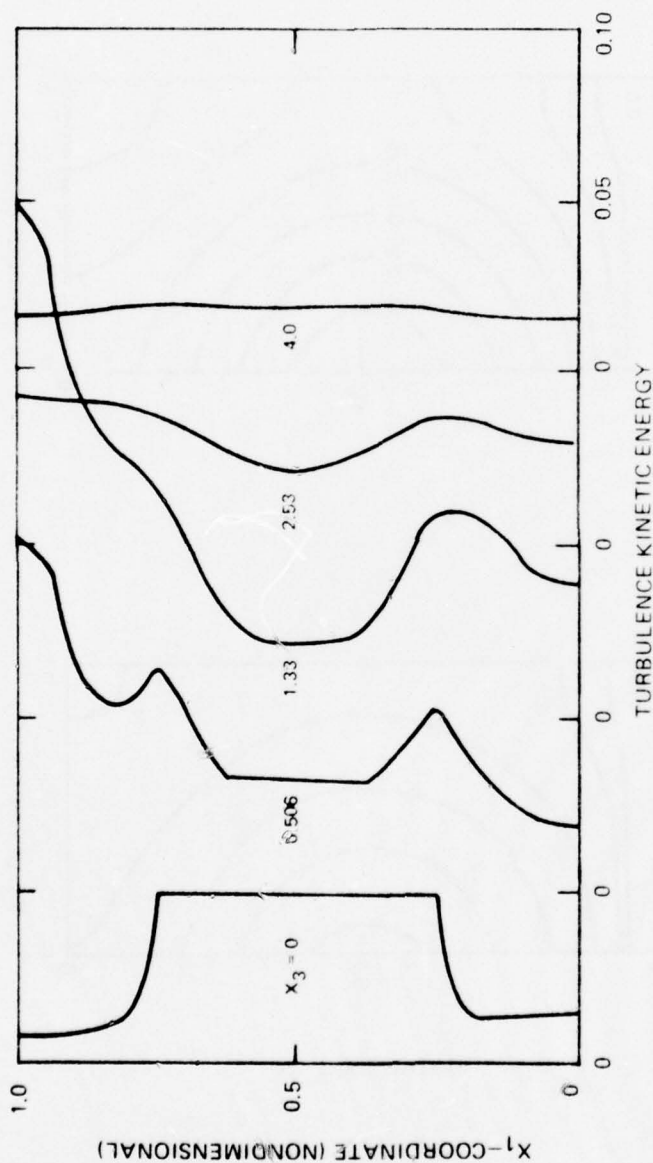


Figure 12. Nondimensional turbulence kinetic energy profiles

SECTION B  $X_1 = 0.5$

$$k_D = 2.544 \times 10^4 \text{ m}^2/\text{s}^2$$

$$L = 0.01905 \text{ m}$$

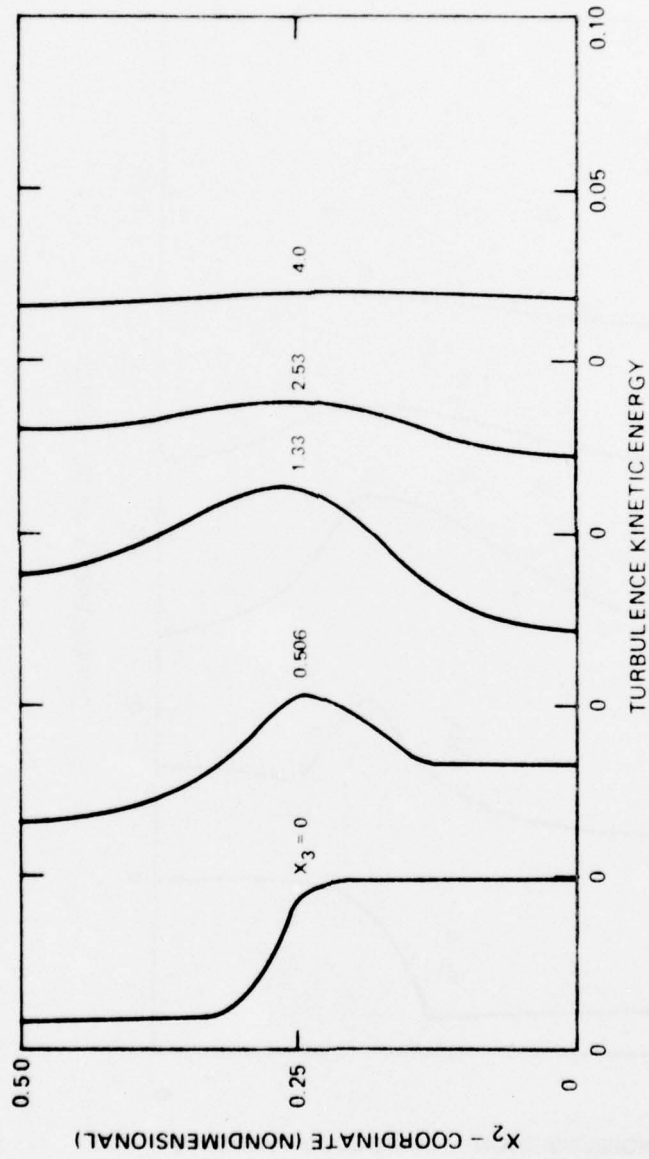


Figure 13. Nondimensional turbulence kinetic energy profiles

SECTION C. DIAGONAL

$$k_D = 2.544 \times 10^4 \text{ m}^2/\text{s}^2$$

$$L = 0.01905 \text{ m}$$

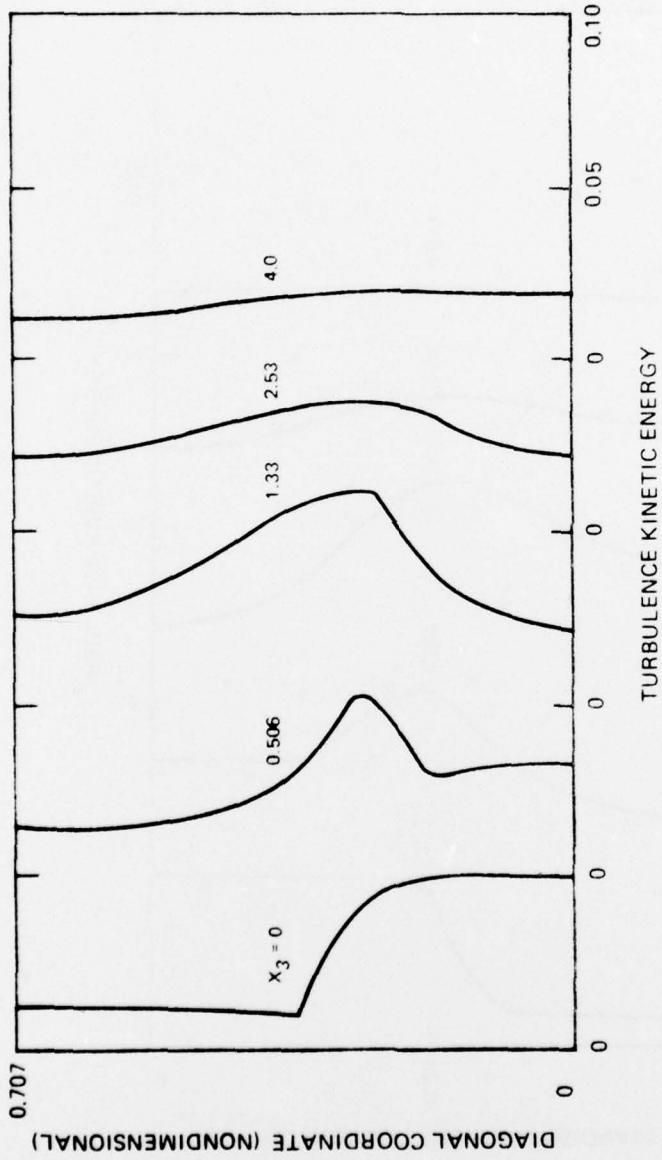


Figure 14. Nondimensional turbulence kinetic energy profiles

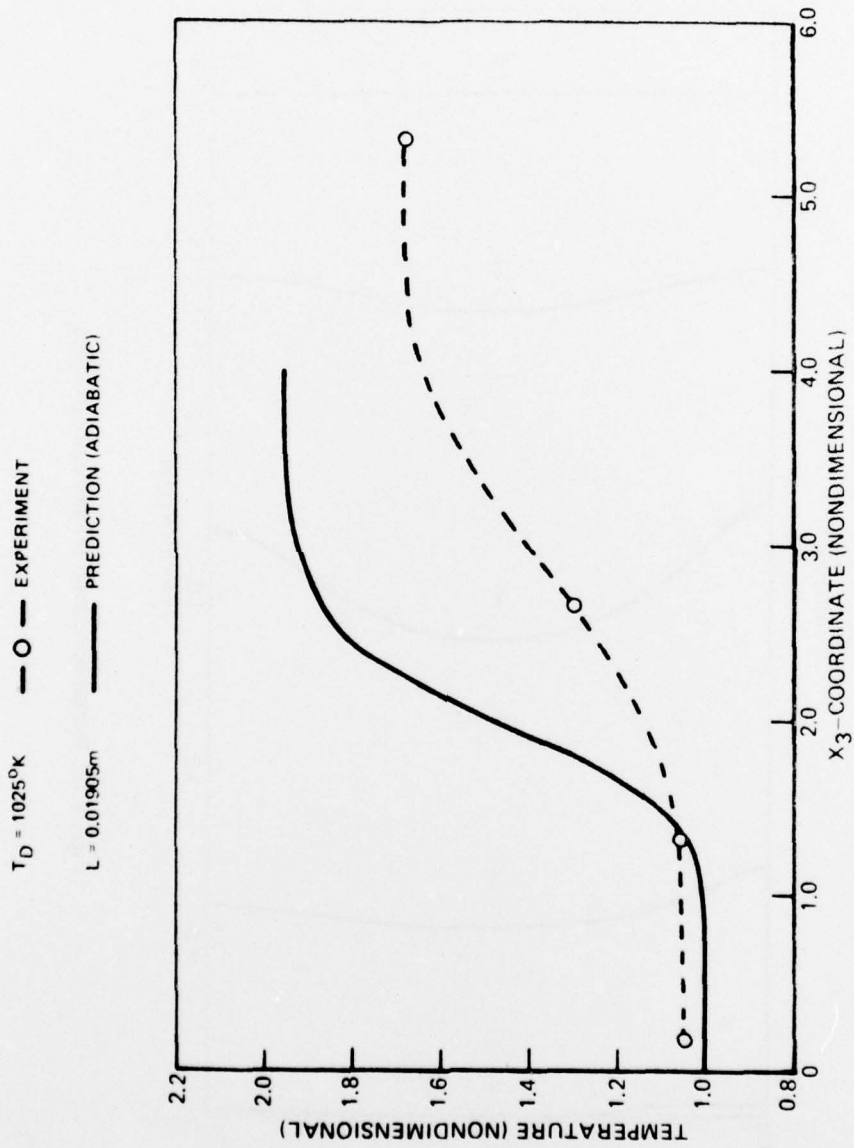


Figure 15. Axial variation of temperature along port centerline ( $X_1 = 0.5$ ,  $X_2 = 0.0$ )

SECTION A:  $X_2 = 0.0$   
 $T_D = 1025^{\circ}\text{K}$   
 $L = 0.01905\text{m}$

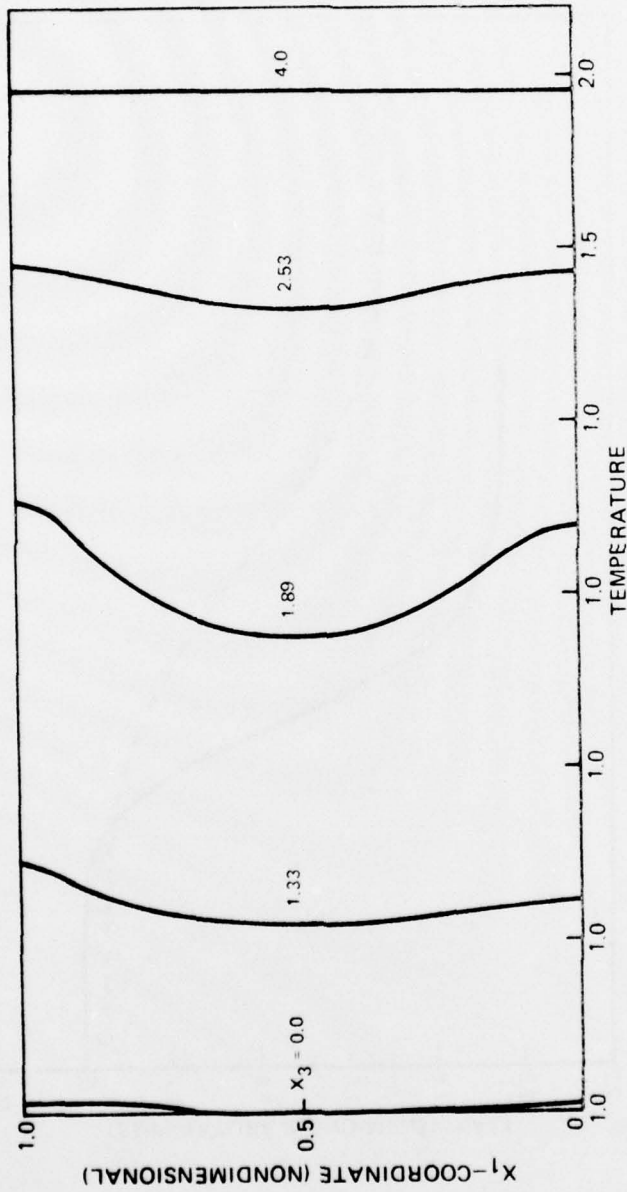


Figure 16. Nondimensional temperature profiles

SECTION B:  $X_1 = 0.5$

$T_D = 1025^\circ\text{K}$

$L = 0.01905\text{ m}$

○ EXPERIMENT  
— PREDICTION

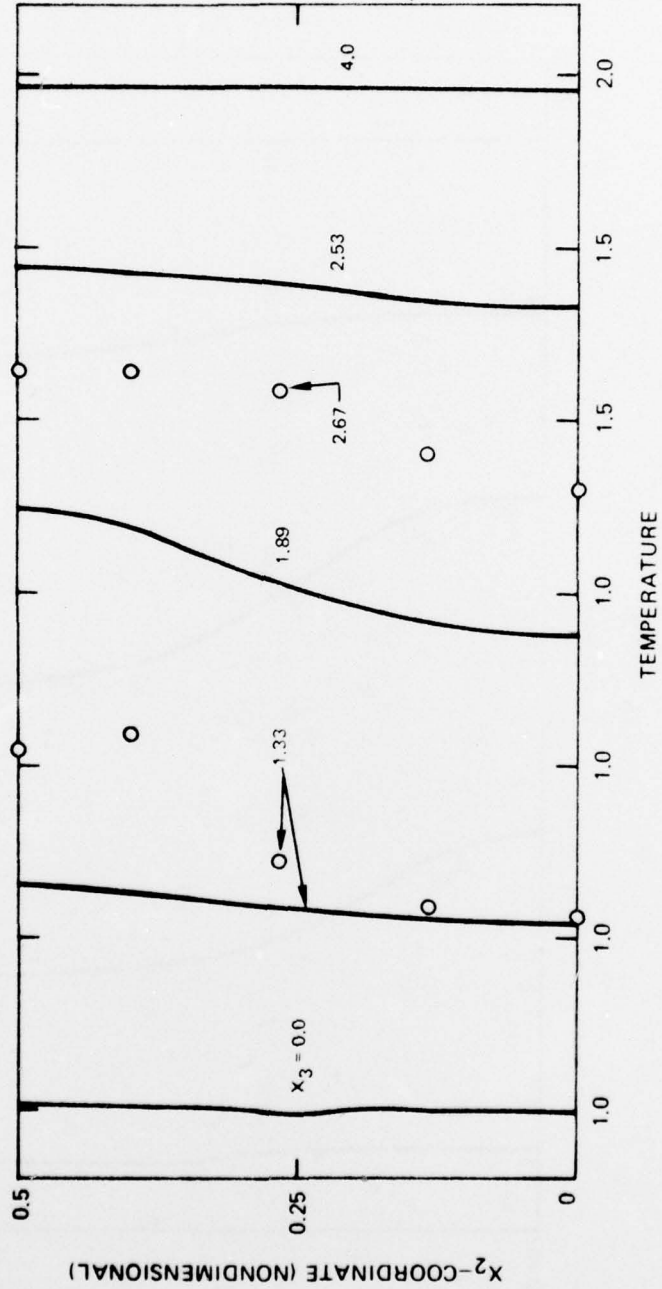


Figure 17. Nondimensional temperature profiles

SECTION C: DIAGONAL

$T_D = 1025^\circ\text{K}$

$L = 0.01905\text{m}$

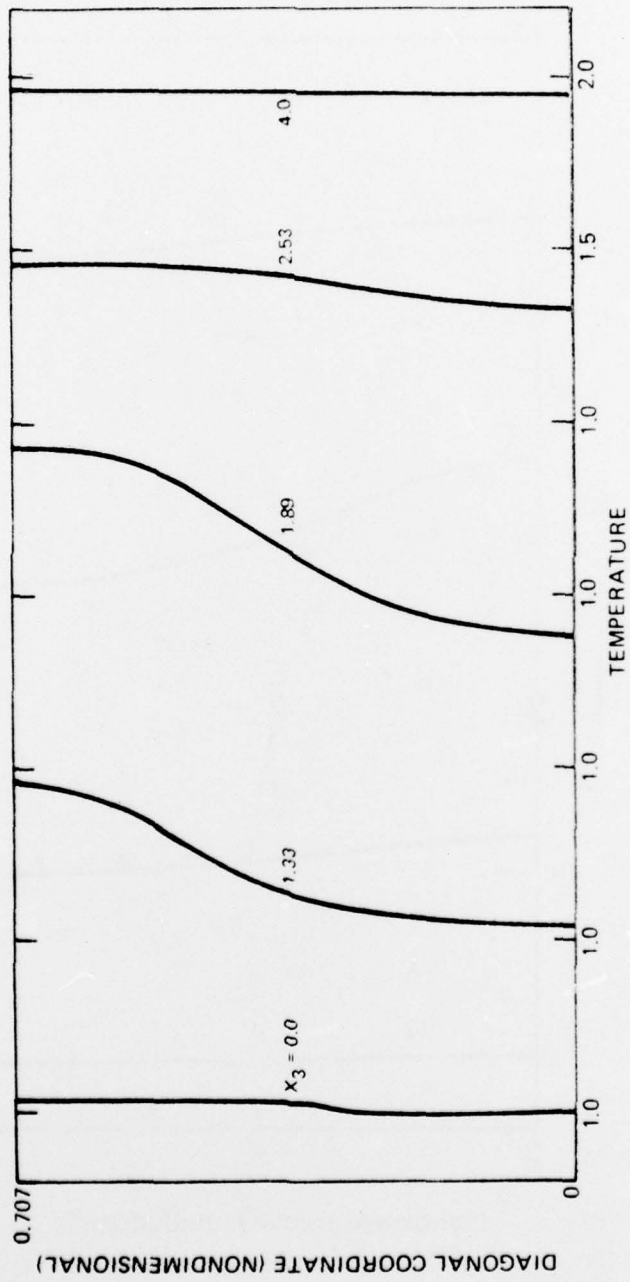


Figure 18. Nondimensional temperature profiles

$T_D = 1025^\circ\text{K}$

$L = 0.01905\text{ m}$

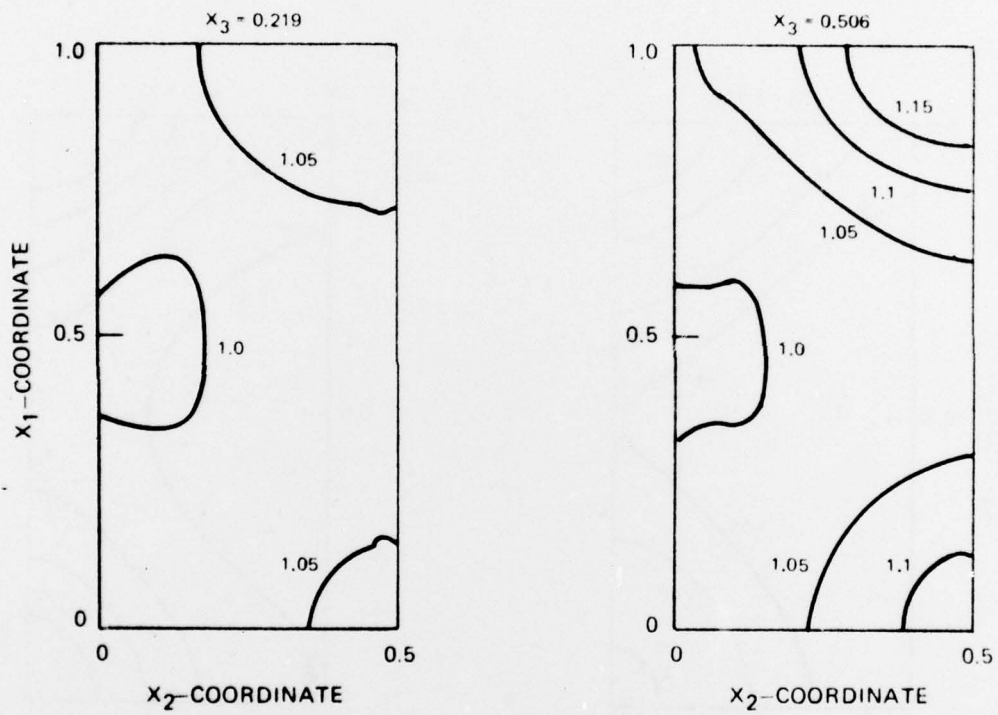


Figure 19. Contours of constant nondimensional temperature in the cross-sectional plane

$T_D = 1025^\circ\text{K}$

$L = 0.01905\text{ m}$

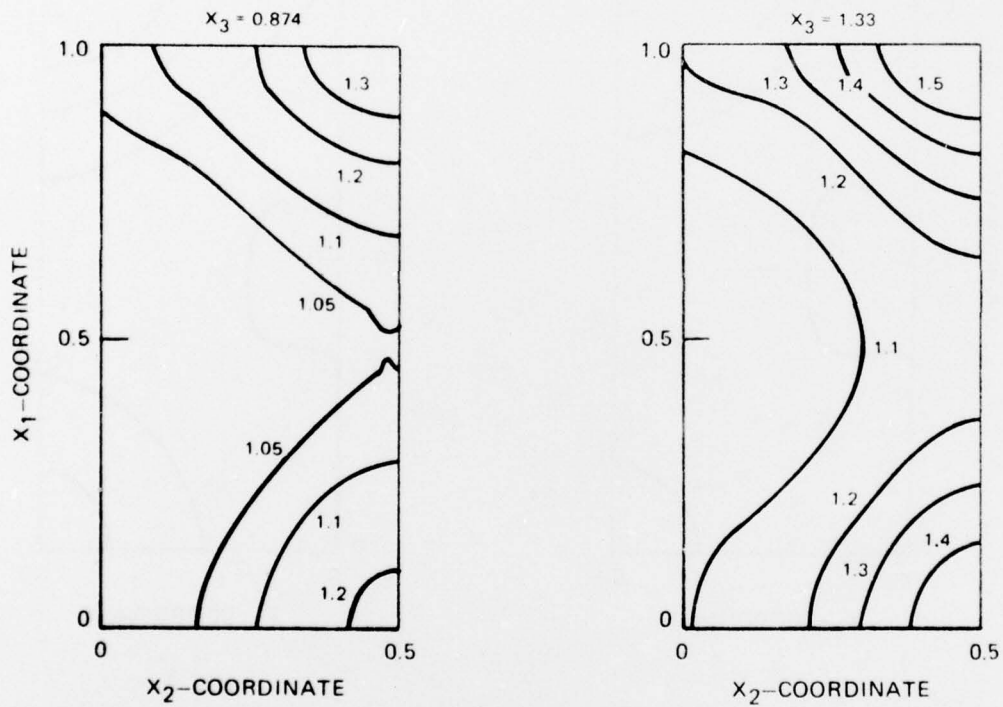


Figure 20. Contours of constant nondimensional temperature in the cross-sectional plane

$T_D = 1025^{\circ}\text{K}$

$L = 0.01905\text{ m}$

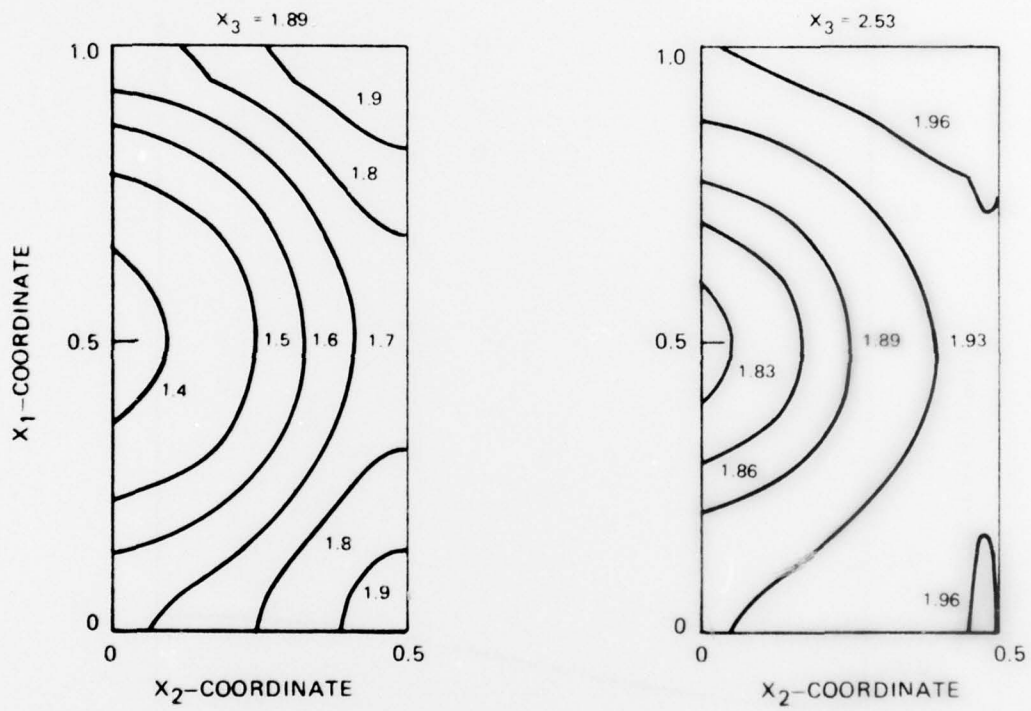


Figure 21. Contours of constant nondimensional temperature in the cross-sectional plane

SECTION B:  $X_1 = 0.5$

—  $X_3 = 4.0$ , PREDICTION  
◇  $X_3 = 2.67$   
□  $X_3 = 4.0$   
△  $X_3 = 5.33$  } EXPERIMENT

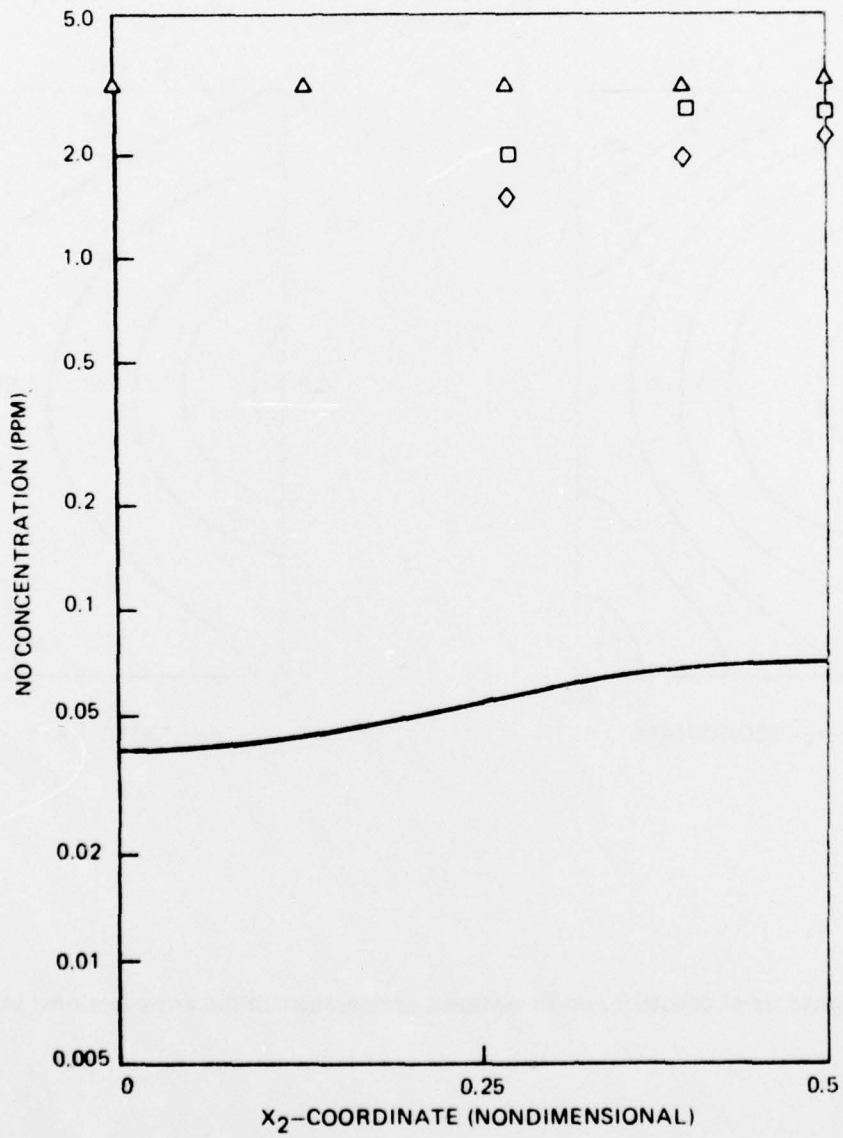


Figure 22. Comparison between predicted and experimental nitric oxide (NO) concentration profiles

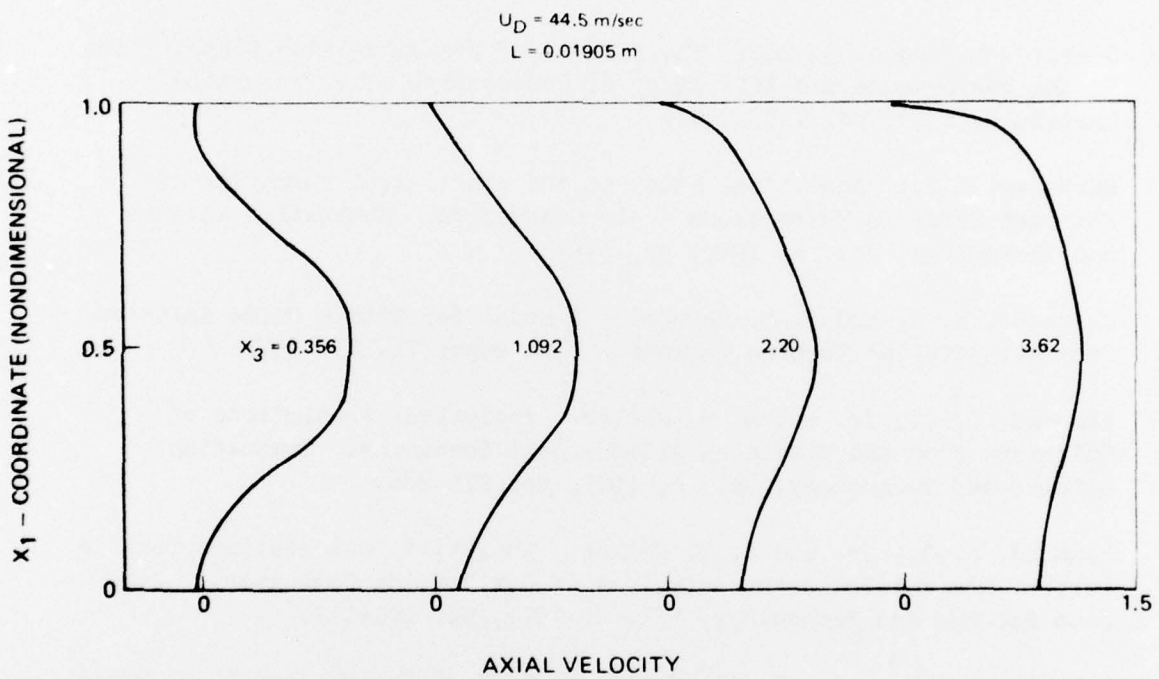


Figure 23. Nondimensional Axial Velocity Profiles for Two-Dimensional FREP Calculation

#### REFERENCES

1. Beer, J. M. and N. A. Chigier: Stability and Combustion Intensity of Pulverized Coal Flames - Effect of Swirl and Impingement. Journal of the Institute of Fuel, December 1969.
2. Beer, J. M. and W. Leucker: Turbulent Flames in Rotating Flow Systems. Paper No. Inst. F-NAFTC-7, North American Fuel Technology Conference, Ottawa, Canada, 1970.
3. Beer, J. M. and J. B. Lee: The Effects of Residence Time Distribution on the Performance and Efficiency of Combustors. The Combustion Institute, 1965, pp. 1187-1202.
4. Marteney, P. J.: Analytical Study of the Kinetics of Formation of Nitrogen Oxide in Hydrocarbon - Air Combustion. Combustion Science and Technology, Vol. 1, 1970, pp. 37-45.
5. Fletcher, R. S. and J. B. Heywood: A Model for Nitric Oxide Emission from Aircraft Gas Turbine Engines. AIAA Paper 71-123, 1971.
6. Hammond, D. C., Jr. and A. M. Mellor: Analytical Predictions of Emissions from and Within an Allison J-33 Combustor. Combustion Science and Technology, Vol. 6, 1973, pp. 279-286.
7. Hammond, D. C., Jr. and A. M. Mellor: Analytical Calculations for the Performance and Pollutant Emissions of Gas Turbine Combustors. Combustion Science and Technology, Vol. 4, 1971, pp. 101-112.
8. Roberts, R., L. D. Aceto, R. Keilback, D. P. Teixeira, and J. M. Bonnell: An Analytical Model for Nitric Oxide Formation in a Gas Turbine Combustion Chamber. AIAA Paper No. 71-715, 1971.
9. Mosier, S. A., R. Roberts, and R. E. Henderson: Development and Verification of an Analytical Model for Predicting Emissions from Gas Turbine Engine Combustors During Low Power Operation. 41st Meeting Propulsion and Energetics Panel of AGARD, 1973.
10. Edelman, R. and C. Economos: A Mathematical Model for Jet Engine Combustor Pollutant Emissions. AIAA Paper No. 71-714, 1971.
11. Gosman, A. D., W. M. Pun, A. K. Runchal, D. B. Spalding, and M. Wolfshtein: Heat and Mass Transfer in Recirculating Flows. Academic Press, New York, 1969.

12. Gosman, A. D. and W. M. Pun: Lecture notes for course entitled "Calculation of Recirculating Flows". Report No. HTS/7412, Department of Mechanical Engineering, Imperial College, London, 1974.
13. Patankar, S. V. and D. B. Spalding: A Calculation Procedure for Heat, Mass and Momentum Transfer in Three-Dimensional Parabolic Flows. Int. J. Heat Mass Transfer, Vol. 15, 1972, p. 1787.
14. Khalil, E. E., D. B. Spalding and J. H. Whitelaw: The Calculation of Local Flow Properties in Two-Dimensional Furnaces. Int. J. Heat Mass Transfer, Vol. 18, 1975, pp. 775-791.
15. Gosman, A. D., F. C. Lockwood and S. A. Syed: Prediction of a Horizontal, Free, Turbulent Diffusion Flame. Proceedings Sixteenth Symposium (International) on Combustion, The Combustion Institute, 1976, to be published.
16. Anasoulis, R. F., H. McDonald and R. C. Buggeln: Development of a Combustor Flow Analysis, Part I: Theoretical Studies. Air Force Aero Propulsion Laboratory Report AFAPL-TR-73-98, Part I, January 1974.
17. Patankar, S. V. and D. B. Spalding: A Computer Model for Three-Dimensional Flow in Furnaces. Proceedings Fourteenth Symposium (International) on Combustion, The Combustion Institute, 1973, pp. 606-614.
18. Patankar, S. V. and D. B. Spalding: Simultaneous Predictions of Flow Pattern and Radiation for Three-Dimensional Flames. Heat Transfer in Flames, edited by N. Afgan and J. Beer, Scripta, Washington, 1974.
19. Gibeling, H. J., H. McDonald and W. R. Briley: Development of a Three-Dimensional Combustor Flow Analysis, Vol. I: Theoretical Studies. Air Force Aero-Propulsion Laboratory Report AFAPL-TR-75-59, Vol. I, July 1975.
20. Briley, W. R. and H. McDonald: An Implicit Numerical Method for the Multidimensional Compressible Navier-Stokes Equations. United Aircraft Research Laboratories Report M911363-6, November 1973.
21. Briley, W. R., H. McDonald and H. J. Gibeling: Solution of the Multidimensional Compressible Navier-Stokes Equations by a Generalized Implicit Method. United Technologies Research Center Report R75-911363-15, January 1976.

22. Launder, B. E. and D. B. Spalding: *Mathematical Models of Turbulence* Academic Press, London, 1972.
23. Harlow, F. H., ed.: *Turbulence Transport Modeling*. AIAA Selected Reprint Series, Vol. XIV, 1973.
24. Launder, B. E.: *Progress in the Modeling of Turbulent Transport*. Notes for Course on Turbulent Recirculating Flows-Prediction and Measurement, Pennsylvania State University, July 1975.
25. Prandtl, L.: *Bericht Uber Untersuchungen Zur Ausgebildeten Turbulenz*. ZAMM, Vol. 5, 1925, p. 136.
26. Patankar, S. V. and D. B. Spalding: *Heat and Mass Transfer in Boundary Layers*. Intertext Books, London, 1970.
27. Maise, G. and H. McDonald: *Mixing Length and Kinematic Eddy Viscosity in a Compressible Boundary Layer*. AIAA Journal, Vol. 6, 1968, pp. 73-80.
28. McDonald, H. and F. J. Camarata: *An Extended Mixing Length Approach for Computing the Turbulent Boundary Layer Development*. Proceedings of the AFOSR-IFP-Stanford Conference on Boundary Layer Prediction, 1968.
29. Williamson, J. W.: *An Extension of Prandtl's Mixing Length Theory*. Applied Mechanics and Fluids Engineering Conference, ASME, June 1969.
30. Lilley, D. G.: *Prediction of Inert Turbulent Swirl Flows*. AIAA Paper No. 72-699, 1972.
31. Van Driest, E. R.: *On Turbulent Flow Near a Wall*. Journal of the Aeronautical Sciences, November 1956.
32. Beer, J. M. and N. A. Chigier: *Combustion Aerodynamics*. Wiley, New York, 1972.
33. Kolmogorov, A. N.: *Equations of Turbulent Motion of an Incompressible Turbulent Fluid*. Izv. Akad. Naut. SSR Ser. Phys. VI, No. 1-2, 56, 1942.
34. Spalding, D. B.: *The Prediction of Two-dimensional, Steady Turbulent Flows*, Imperial College, Heat Transfer Section Report EF/TN/A/16, 1969.
35. Saffman, P. G.: *A Model for Inhomogenous Turbulent Flow*. Proc. Roy. Soc. Ser. A317, 1970, p. 417.
36. Launder, B. E. and D. B. Spalding: *The Numerical Computation of Turbulent Flows*. Computer Methods in Applied Mechanics and Engineering, Vol. 3, 1974, p. 269.

37. Jones, W. P. and B. E. Launder: The Prediction of Laminarization with a Two-equation Model of Turbulence. *Int. J. Heat Mass Transfer*, Vol. 15, 1972, p. 301.
38. Walz, A.: *Boundary Layers of Flow and Temperature*. M.I.T. Press, Cambridge, Massachusetts, 1969, p. 115.
39. Roach, P. J.: *Computational Fluid Dynamics*. Hermosa Publishers, Albuquerque, 1972.
40. Orszag, S. A. and M. Israeli: Numerical Simulation of Viscous Incompressible Flows. *Annual Reviews in Fluid Mechanics*, Vol. 6, 1974, p. 281.
41. Mitchell, A. R.: *Computational Methods in Partial Differential Equations*. Wiley, New York, 1969.
42. Wormeck, J. J. and D. T. Pratt: Computer Modeling of Combustion in a Longwell Jet-Stirred Reactor. *Proceedings Sixteenth Symposium (International) on Combustion*, The Combustion Institute, 1976, to be published.
43. Hutchinson, P., E. E. Khalil and J. H. Whitelaw: The Calculation of Wall Heat Transfer Rate and Pollution Formation in Axisymmetric Furnaces. Presented at Fourth Members Conference, International Flame Research Foundation, Ijmuiden, Holland, May 1976.